Repubblica e Cantone Ticino
Dipartimento del territorio

Results from the participation of Switzerland to the International Cooperative Programme on Assessment and Monitoring Effects of Air Pollution on Rivers and Lakes (ICP Waters)

Biannual report 2023-2024

Ufficio del monitoraggio ambientale
Sandra Steingruber
Telefono: 091 814 29 30
e-mail: sandra.steingruber@ti.ch
Bellinzona, 25.8.2025

Chemical water analysis:	Laboratorio SPAAS, DT Canton Ticino
Chemical sampling:	Laboratorio SPAAS, DT Canton Ticino Adriano Bolgé, Anna Bonetti, Dorina Genucchi, Mattia Scolari, Lara Lucini, MeteoSvizzera Locarno Monti, Ofima
Sampling and determination of macroinvertebrates	Chiara Caissutti Pradella, Pierre Marle (chironomids)

Content

Summary

Established in 1985 under the Convention on Long-Range Transboundary Air Pollution (CLRTAP) of the United Nations Economic Commission for Europe (UNECE), the ICP Waters program monitors the effects of air pollution, particularly acidification from sulfur and nitrogen emissions, on surface waters across Europe and North America. Switzerland joined the program in 2000, represented by the Swiss Federal Office for the Environment with support from Canton Ticino.

The study area located in the Southern Alps (Canton Ticino, Switzerland), is highly sensitive to acidification due to its base-poor geology, particularly gneiss, and is significantly impacted by long-range transboundary air pollution from the Po Plain. To assess these effects, water chemistry monitoring is conducted in 20 acid-sensitive high-altitude lakes and in the Verzasca River, with wet deposition measured at seven sites. Macroinvertebrates are sampled as bioindicators in two of the most acidic lakes.

The monitoring data highlight ongoing trends in atmospheric deposition and its impact on water chemistry.

Ion concentrations in precipitation from anthropogenic sources (SO_4, NO_3, NH_4) decrease with increasing latitude and altitude, reflecting the influence of pollution transport from the Po Plain and the distance from pollution sources. Due to significant reductions in SO_2 emissions, SO_4 depositions experienced a sharp decline, particularly between the 1990s and 2010. Similarly, decreased NO_x emissions led to reductions in NO_3 depositions, especially from 2000 to 2015. NH_4 depositions also showed a slight but consistent decrease at most sites. As a consequence, total acidifying deposition decreased at all sites.

Consistent with trends observed atmospheric depositions, concentrations of SO_4 and NO_3 decreased, while total alkalinity (TAlk) increased in most lakes. In lakes significantly influenced by thawing cryospheric features (rock glaciers), both SO_4 and base cation concentrations rose, though the upward trend in TAlk remained relatively unchanged. Recent trends seem to suggest that climate change may be accelerating the release of DOC and Al, particularly in lake catchments located at lower altitudes.

Likewise, the long-term decline in SO_4 and NO_3 concentrations in river Verzasca has resulted in higher TAlk and pH levels. Additionally, a slight increase in SiO_2 concentrations has been observed, likely driven by intensified physical and chemical weathering processes associated with climate change.

Since the ultimate goal of emission control programmes is biological recovery—such as the return of acid-sensitive species that have disappeared—and the restoration of biological functions impaired by acidification, macroinvertebrates have been studied as bioindicators in two of the most acidic lakes: Lago del Starlaresc da Sgiof and Lago Tomé. However, no clear signs of biological recovery have been observed to date. None of the analysed biological indicators—including the total number of taxa, the number of EPT taxa, chironomid taxa, or the relative abundance of EPT taxa—have shown an increasing trend over time, nor has there been evidence of reappearance of more acid-sensitive species

Riassunto

Istituito nel 1985 nell'ambito della Convenzione sull'inquinamento atmosferico transfrontaliero a lunga distanza (CLRTAP) della Commissione economica per l'Europa delle Nazioni unite (UNECE), il programma ICP Waters monitora gli effetti dell'inquinamento atmosferico, in particolare dell'acidificazione causata dalle emissioni di zolfo e azoto, sulle acque superficiali in Europa e Nord America. La Svizzera ha aderito al programma nel 2000, rappresentata dall'Ufficio federale dell'ambiente (UFAM) con il supporto del Canton Ticino.

L'area di studio, situata nelle Alpi meridionali (Canton Ticino, Svizzera), è altamente sensibile all'acidificazione a causa della sua geologia povera di rocce basiche, in particolare gneiss, ed è significativamente influenzata dall'inquinamento atmosferico transfrontaliero a lunga distanza proveniente dalla Pianura Padana. Per valutare questi effetti, il monitoraggio della chimica delle acque viene effettuato in 20 laghi d'alta quota sensibili all'acidificazione e nel fiume Verzasca, mentre le deposizioni umide vengono misurate in sette siti. Inoltre, i macroinvertebrati sono campionati come bioindicatori in due dei laghi più acidi.

I dati di monitoraggio evidenziano tendenze significative nelle deposizioni atmosferiche e il loro impatto sulla chimica delle acque.

Le concentrazioni degli ioni di origine antropica (SO_4, NO_3, NH_4) diminuiscono con l'aumentare della latitudine e dell'altitudine, riflettendo l'influenza del trasporto di inquinanti dalla Pianura Padana e la distanza dalle fonti di inquinamento. A causa della significativa riduzione delle emissioni di SO_2, le deposizioni di SO_4 hanno subito un netto calo, in particolare tra gli anni '90 e il 2010. Analogamente, la diminuzione delle emissioni di NO_x ha portato a una riduzione delle deposizioni di NO_3, soprattutto tra il 2000 e il 2015. Anche le deposizioni di NH_4 hanno mostrato un leggero ma costante calo nella maggior parte dei siti. Di conseguenza la deposizione acidificante totale è diminuita in tutti i siti.

In linea con le tendenze osservate nelle deposizioni atmosferiche, le concentrazioni di SO_4 e NO_3 sono diminuite, mentre l'alcalinità totale (TAlk) è aumentato nella maggior parte dei laghi. Nei laghi significativamente influenzati dallo scioglimento della criosfera (ghiacciai rocciosi), sia le concentrazioni di SO_4 che dei cationi basici sono aumentate, senza tuttavia modificare significativamente il trend crescente del TAlk. Trend recenti sembrano indicare

che il cambiamento climatico potrebbe accelerare il rilascio di DOC e Al, in particolare nei bacini lacustri situati a quote più basse.

Analogamente, la diminuzione delle concentrazioni di SO_4 e NO_3 nel fiume Verzasca ha portato a un aumento dei livelli di TAlk e pH. Inoltre, è stato osservato un leggero aumento delle concentrazioni di SiO_2, probabilmente legato all'intensificazione dei processi di erosione e degradazione chimica dovuta ai cambiamenti climatici.

Poiché l'obiettivo finale dei programmi di controllo delle emissioni è il recupero biologico—ossia il ritorno delle specie sensibili all'acidificazione che sono scomparse—e il ripristino delle funzioni biologiche compromesse dall'acidificazione, i macroinvertebrati sono stati studiati come bioindicatori in due dei laghi più acidi: il Lago del Starlaresc da Sgiof e il Lago Tomé. Tuttavia, ad oggi non sono stati osservati chiari segnali di recupero biologico. Nessuno degli indicatori biologici analizzati—tra cui il numero totale di taxa, il numero di taxa EPT, i taxa dei chironomidi o l'abbondanza relativa dei taxa EPT—ha mostrato un trend in aumento nel tempo, né vi è evidenza della ricomparsa di specie più sensibili all'acidificazione.

1 Introduction

The International Cooperative Programme on Assessment and Monitoring Effects of Air Pollution on Rivers and Lakes (ICP Waters) was established in 1985 under the United Nations Economic Commission for Europe's Convention on Long-Range Transboundary Air Pollution (CLRTAP). It was initiated in response to the early evidence that freshwater acidification was a direct consequence of sulphur emissions.

The monitoring programme is designed to assess, on a regional basis, the degree and geographical extent of the impact of atmospheric pollution, in particular acidification on surface waters. The monitoring data provide a basis for documenting effects of long-range transboundary air pollutants on aquatic chemistry and biota. An additional important programme activity is to contribute to quality control and harmonization of monitoring methods.

The Programme is planned and coordinated by a Task Force under the leadership of Norway. Up to now data from about 20 countries in Europe and North America are available in the database of the Programme Centre. Switzerland joined the Programme in 2000 on behalf of the Swiss Federal Office for the Environment with the support of Canton Ticino.

2 Study sites

The study area is located in the Southern Alps, within the Canton Ticino, Switzerland. Precipitation in this region is primarily determined by warm, humid air masses originating from the Mediterranean Sea, which travel across the Po Plain before colliding with the Alps. The north-western part of the canton is predominantly composed of base-poor rocks, particularly gneiss. As a result, the soils and freshwaters systems in this region are highly sensitive to acidification.

To evaluate the impact of long-range transboundary air pollution, monitoring of water chemistry has been conducted in 20 acid-sensitive high-altitude lakes and in the Verzasca river at Sonogno. Wet deposition has been measured at seven sampling sites distributed across Ticino. Additionally, macroinvertebrates, serving as bioindicators, were sampled in two of the most acidic lakes (STA, TOM, see Tab. 2.3).

The lake watersheds consist primarily of bare rock, with vegetation restricted to small patches of Alpine meadows. The Alpine lakes, located at altitude between 1690 m and 2590 m, are characterized by intense solar radiation, a short growing season, a long period of ice coverage and low nutrient concentrations. In contrast, the sampling points of river Verzasca is situated at lower elevation (918 m). Do to its larger catchment area with greater buffer capacity the Verzasca river is less sensitive to acidification.

The geographic distribution of the sampling sites (wet deposition, river and lakes) are shown in Fig. 2.1, while their key geographic and morphometric parameters are summarized in Tab. 2.1, 2.2 and 2.3.

Figure 2.1 Sampling sites (Relief map: © Swisstopo)

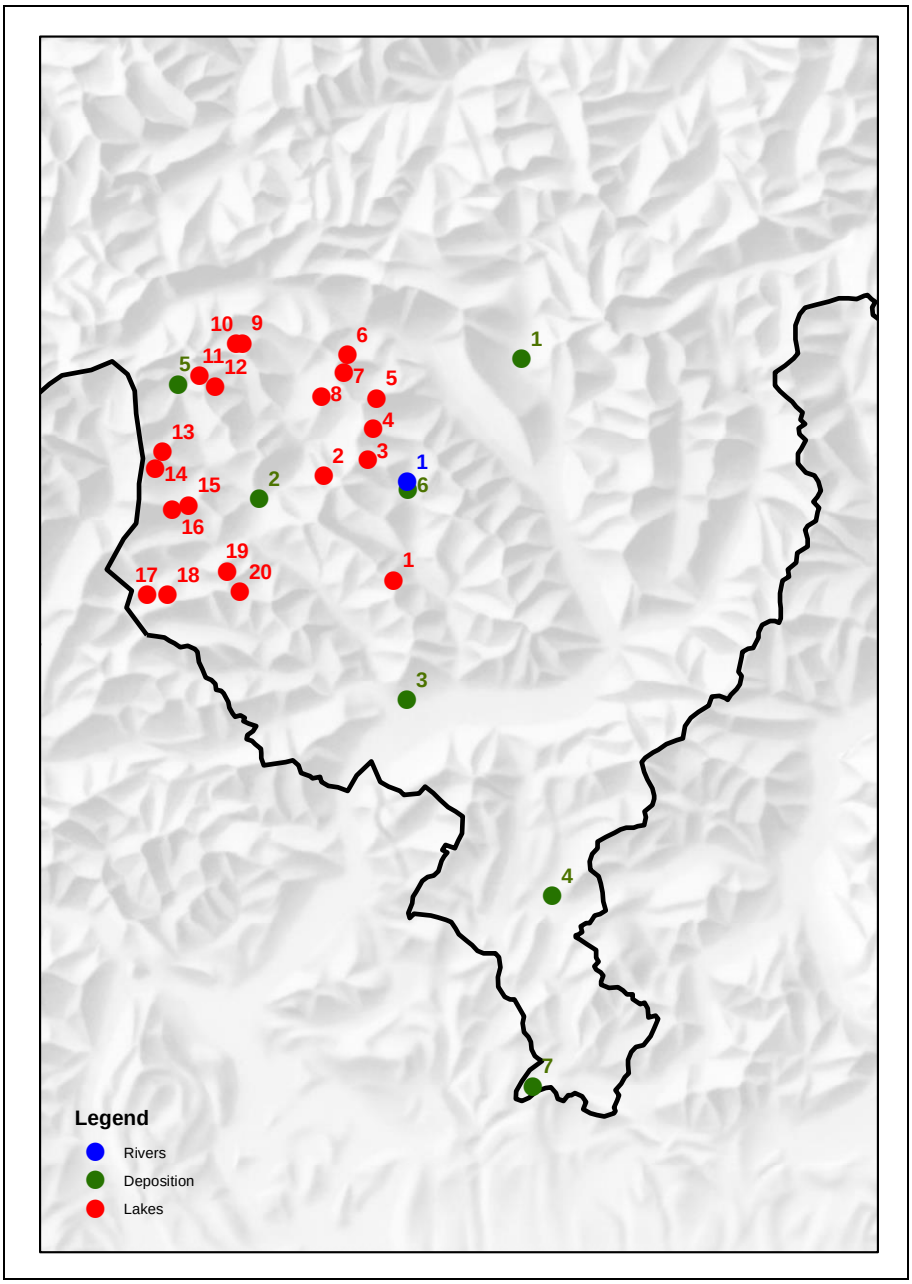

Table 2.1 Geographic and morphometric parameters of the wet deposition sampling sites

Sampling site number	Code	Sampling site	CH1903 LV03 (m)		WGS84		Altitude
			Longitude	Latitude	Longitude	Latitude	m a.s.l.
1	ACQ	Acquarossa	714998	146440	8°56'12''	46°27'41''	575
2	BIG	Bignasco	690205	132257	8°59'17''	46°00'32''	443
3	LOC	Locarno Monti	704160	114350	8°47'17''	46°10'27''	366
4	LUG	Lugano	717880	95870	8°57'18''	46°00'24''	273
5	ROB	Robiei	682540	143984	8°30'51''	46°26'43''	1890
6	SON	Sonogno	704250	134150	8°47'14''	46°21'05''	918
7	STA	Stabio	716040	77970	8°55'52''	45°51'36''	353

Table 2.2 Geographic and morphometric parameters of the studied river sites

River number	River code	River name	Sampling site	CH1903 LV03 (m)		WGS84		Altitude	Catchment area
				Longitude	Latitude	Longitude	Latitude	m a.s.l	km^2
1	VER	VER	Sonogno	704200	134825	8°47'33''	46°21'24'	918	ca. 27

Table 2.3 Geographic and morphometric parameters of the studied lakes

Lake number	Lake code	Lake name	CH1903 LV03 (m)		WGS84		Altitude	Catchment area	Lake area	Max depth
			Longitude	Latitude	Longitude	Latitude	m a.s.l.	ha	ha	m
1	STA	Lago del Starlaresc da Sgiof	702905	125605	8°46'25''	46°16'26''	1875	23	1.1	6
2	TOM	Lago di Tomè	696280	135398	8°41'23''	46°21'47''	1692	294	5.8	38
3	POR	Lago dei Porchieirsc	700450	136888	8°44'39''	46°22'33''	2190	43	1.5	7
4	BAR	Lago Barone	700975	139813	8°45'06''	46°24'07''	2391	51	6.6	56
5	GAR	Laghetto Gardiscio	701275	142675	8°45'22''	46°45'22''	2580	12	1.1	10
6	LEI	Lago della Capannina Leit	698525	146800	8°43'17''	46°27'55''	2260	52	2.7	13
7	MOR	Lago di Morghirolo	698200	145175	8°43'00''	46°27'03''	2264	166	11.9	28
8	MOG	Lago di Mognòla	696075	142875	8°41'19''	46°25'49''	2003	197	5.4	11
9	INF	Laghetto Inferiore	688627	147855	8°35'34''	46°28'34''	2074	182	5.6	33
10	SUP	Laghetto Superiore	688020	147835	8°35'05''	46°28'34''	2128	125	8.3	29
11	NER	Lago Nero	684588	144813	8°32'22''	46°26'58''	2387	72	12.7	68
13	FRO	Lago della Froda	686025	143788	8°33'29''	46°26'24''	2363	67	2.0	17
14	ANT	Laghetto d'Antabia	681038	137675	8°29'32''	46°23'08''	2189	82	6.8	16
15	CRO	Lago della Crosa	680375	136050	8°28'60''	46°22'16''	2153	194	16.9	70
16	ORS	Lago d'Orsalìa	683513	132613	8°31'24''	46°20'23''	2143	41	2.6	16
17	SCH	Schwarzsee	681963	132188	8°30'11''	46°20'10''	2315	24	0.3	7
18	POZ	Laghi dei Pozzöi	679613	124200	8°28'17''	46°15'52''	1955	33	1.1	4
19	SFI	Lago di Sfille	681525	124213	8°29'46''	46°15'52''	1909	63	2.8	12
20	SAS	Lago di Sascòla	687175	126413	8°34'11''	46°17'01''	1740	90	3.2	5
21	ALZ	Lago d'Alzasca	688363	124488	8°35'05''	46°15'58''	1855	110	10.4	40

3 Climatic parameters during 2023-2024

In 2023 and 2024, Ticino experienced particularly warm climatic conditions. The regional average annual temperature exceeded the 1991-2020 norm by 1.4 °C in 2023 and by 1.3 °C in 2024, following the record-breaking year of 2022, which was 1.5 °C above the norm (MeteoSwiss 2024, 2025). The monthly norm values were also exceeded in most months (Fig. 3.1)

Precipitation patterns during 2023 and 2024 varied across southern Alpine sites, with annual totals slightly below the 1991-2020 norm in 2023 and slightly above in 2024 (Fig. 3.2). However, monthly values often deviated significantly from the norm. Winter 2022/2023 and spring 2023 were characterized by below-average precipitation, extending a severe drought that had persisted in the region for two years. This was followed by intense rainfall in summer 2023, particularly in northern Ticino, and again in spring 2024. In June 2024, the alpine village of Fontana in Val Bavona was struck by a major landslide, attributed to high-altitude permafrost melting due to climate change. The months of July, August, November, and December 2024 were again exceptionally dry.

In summary, Ticino has experienced above-average temperatures and extreme weather events over the past two years, underscoring the ongoing impact of climate change on the region.

Figure 3.1 Monthly mean (2023-2024) and yearly mean (1991-2023) temperature deviation from the norm value (1991-2020) at the wet deposition sampling sites with MeteoSwiss climate data in Canton Ticino. Site acronym as defined in Table 2.1

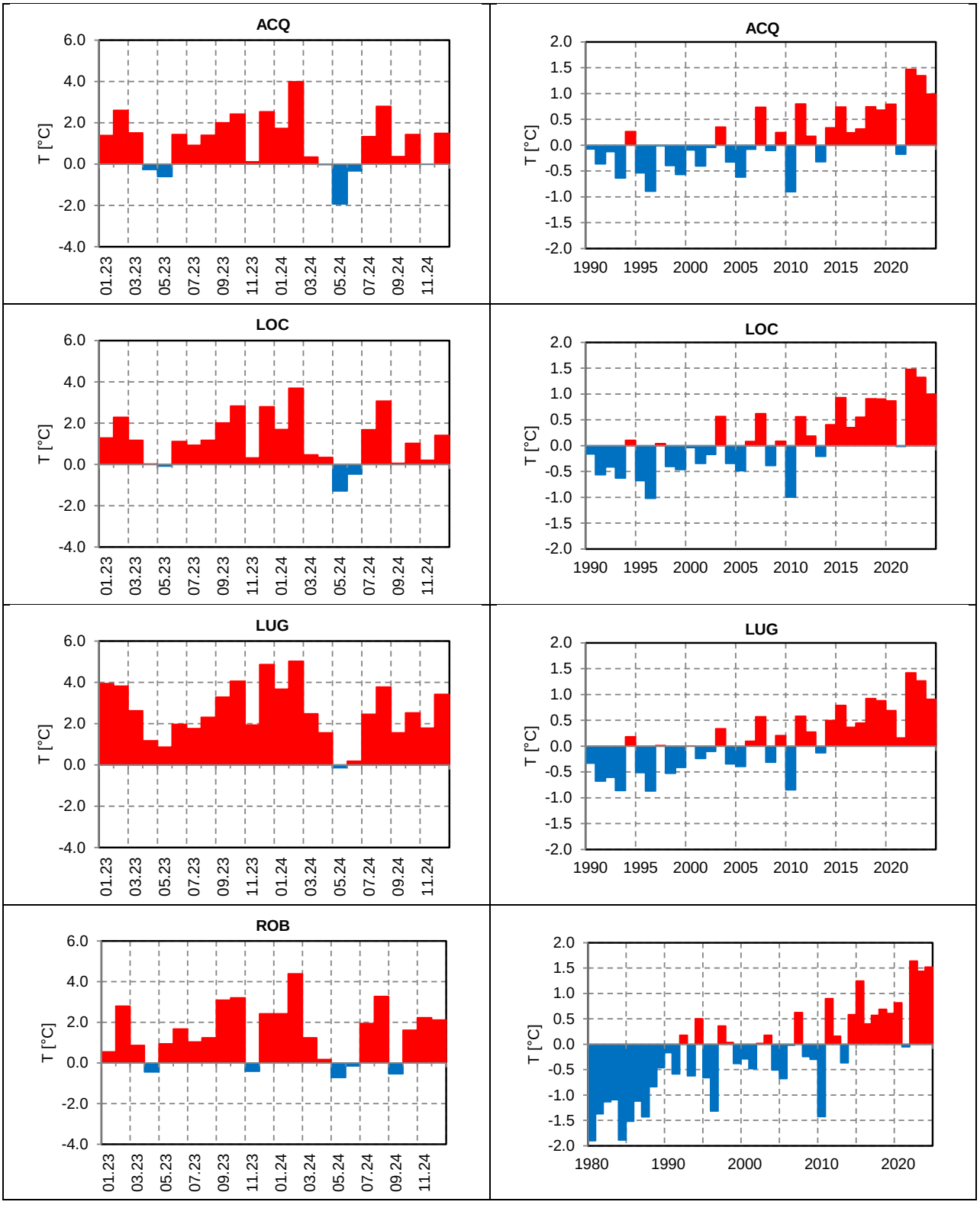

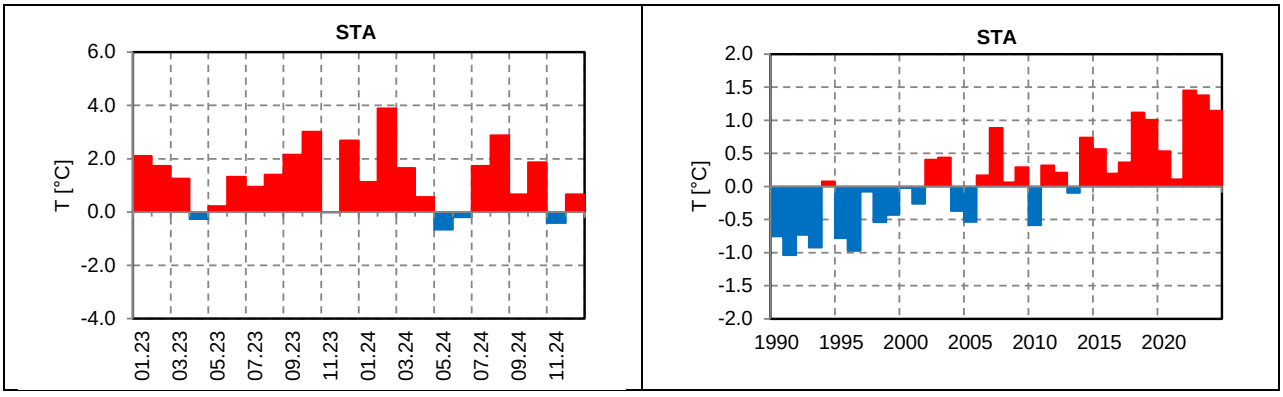
STA
T [°C]
6.0
4.0
2.0
0.0
-2.0
-4.0
01.23
03.23
05.23
07.23
09.23
11.23
01.24
03.24
05.24
07.24
09.24
11.24
STA
T [°C]
2.0
1.5
1.0
0.5
0.0
-0.5
-1.0
-1.5
-2.0
1990
1995
2000
2005
2010
2015
2020

Figure 3.2 Monthly (2023-2024) and yearly (1991-2023) deviation in mm from the norm value (1991-2020) at the wet deposition sampling sites with MeteoSwiss climate data in Canton Ticino. Site acronym as defined in Table 2.1

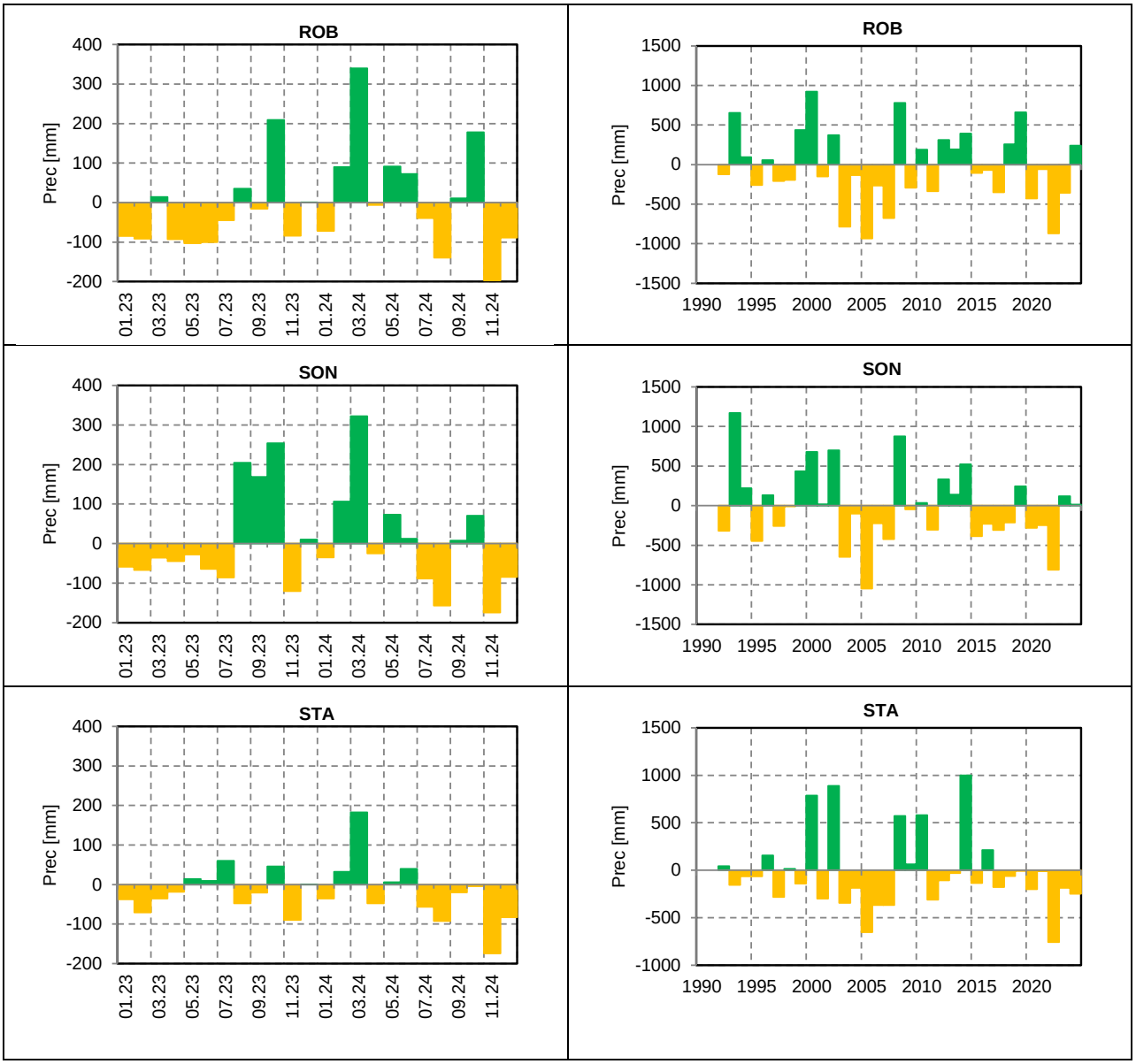
ROB
Prec [mm]
400
300
200
100
0
-100
-200
01.23
03.23
05.23
07.23
09.23
11.23
01.24
03.24
05.24
07.24
09.24
11.24
ROB
Prec [mm]
1500
1000
500
0
-500
-1000
-1500
1990
1995
2000
2005
2010
2015
2020
SON
Prec [mm]
SON
Prec [mm]
STA
Prec [mm]
STA
Prec [mm]

4 Water chemistry analysis

4.1 Introduction

Acid deposition in acid-sensitive areas can cause acidification of surface waters and soils. The north-western part of Canton Ticino is particularly vulnerable to acidification due to its specific lithology (base-poor rocks, primarily gneiss) and high altitudes, (thin soil layer and low temperatures), that limit the buffer capacity.

Acidification can be defined as a reduction of the alkalinity or acid neutralizing capacity (ANC) of soils or waters. Alkalinity is the result of complex interactions between wet and dry deposition, soil and bedrocks of the watershed and biologic processes within a watershed. A commonly used threshold for assessing surface water acidification is an alkalinity (or ANC) of 20 µeq/l, often set based on the responses of fish and invertebrates to acidification (CLRTAP 2023). Indeed, critical loads of acidity for Swiss Alpine lakes have been calculated using this ANC (Posch et al. 2007).

Since concentrations of soluble aluminium begin to rise at pH values below approximately 6.3, it is generally assumed that first signs of acidification-related changes in biological communities appear, when pH drops below 6 (Wright et al. 1975).

4.2 Sampling methods

Rainwater has been collected weekly using wet-only samplers. The first of these samplers was installed at LOC in 1988, followed by additional samplers in 1989 (LUG), in 1990 (ACQ, STA), in 1996 (ROB), and in 2001 (BIG, SON). The altitudes of these sampling sites range from 353 and 1890 m a.s.l.

Between the 1980s and 1990's, surface water of a total of 62 lakes was sampled irregularly. From 2000 a subset of 20 acid-sensitive lakes has been monitored annually:

- From 2000 to 2005: Twice a year - once at beginning of summer, once in autumn).
- From 2006 to 2018: Three times a year - once at the beginning of summer, twice in autumn.
- From 2019 onward: Twice a year in autumn.

The river Verzasca has been sampled monthly since 2000.

4.3 Analytical methods

The measured parameters, conservation methods, analytical techniques, and quantification limits are summarized in Tab. 4.1. The data quality was assured by regular participation in national and international intercalibration tests.

Additionally, data were only accepted if the met the quality criteria outlined in the ICP Waters programme manual (Gundersen 2025) - specifically, a consistent ionic balance and agreement between measured and calculated conductivity.

Furthermore, outlier detection methods were applied. When available, dissolved concentrations (e.g. metals) were compared to total concentrations to validate analytical results.

Table 4.1 Measured parameters, conservation methods, analytical methods, quantification limits. CA, PC, GF, PP stay for cellulose acetate, polycarbonate, glass fibre and polypropylene, respectively

Parameter	Acronym	Filtration	Conservation	Method	Limit of quantification
pH		No	No	potentiometry	0.02
conductivity	Cond	No	No	potentiometry	1 $\mu S\ cm^{-1}$
Gran alkalinity	TAlk	No	No	potentiometry	0.001 meq l^{-1}
calcium	Ca	CA filter	PP bottle, 4°C	ion cromatography	0.06 mg l^{-1}
magnesium	Mg	CA filter	PP bottle, 4°C	ion cromatography	0.01 mg l^{-1}
sodium	Na	CA filter	PP bottle, 4°C	ion cromatography	0.01 mg l^{-1}
potassium	K	CA filter	PP bottle, 4°C	ion cromatography	0.08 mg l^{-1}
ammonium	NH_4	CA filter	PP bottle, 4°C	ion chromatography (precipitations)	0.030 mg N l^{-1}
ammonium	NH_4	CA/GF filter	PP bottle, 4°C	UV/VIS (lakes, rivers)	0.012 mg N l^{-1}
sulphate	SO_4	CA/GF filter	PP bottle, 4°C	ion cromatography	0.08 mg l^{-1}
nitrate	NO_3	CA/GF filter	PP bottle, 4°C	ion cromatography	0.02 mg N l^{-1}
nitrite	NO_2	CA/GF filter	PP bottle, 4°C	ion cromatography	0.2 μg N l^{-1}
chloride	Cl	CA/GF filter	PP bottle, 4°C	ion cromatography	0.1 mg l^{-1}
phosphate	PO_4	CA/GF filter	PP bottle, 4°C	ion cromatography	2 μg P l^{-1}
total phosphorus	TP	No	glass bottle, persulphate mineralisation	UV/VIS	32 μg P l^{-1}
silica	SiO_2	CA/GF filter	PP bottle, 4°C	ICP-MS	0.06 mg SiO_2 l^{-1}
total nitrogen	TN	No	glass bottle, persulphate mineralisation	UV/VIS	0.15 mg N l^{-1}
dissolved organic carbon	DOC	PC filter	brown glass bottle	IR-catalytic oxidation and combustion	0.05 mg C l^{-1}
reactive Al	RAl	PC filter	acid washed PP bottle, +HNO_3, 4°C	ICP-MS	1.0 μg l^{-1}
not filtered Al	TAl	No	acid washed PP bottle, +HNO_3, 4°C	ICP-MS	1.0 μg l^{-1}
filtered Pb	Pb_{fil}	PC filter	acid washed PP bottle, +HNO_3, 4°C	ICP-MS	0.1 μg l^{-1}
not filtered Pb	Pb_{tot}	No	acid washed PP bottle, +HNO_3, 4°C	ICP-MS	0.1 μg l^{-1}
filtered Cd	Cd_{fil}	PC filter	acid washed PP bottle, +HNO_3, 4°C	ICP-MS	0.1 μg l^{-1}
not filtered Cd	Cd_{tot}	No	acid washed PP bottle, +HNO_3, 4°C	ICP-MS	0.1 μg l^{-1}
filtered Cu	Cu_{fil}	PC filter	acid washed PP bottle, +HNO_3, 4°C	ICP-MS	0.1 μg l^{-1}
not filtered Cu	Cu_{tot}	No	acid washed PP bottle, +HNO_3, 4°C	ICP-MS	0.1 μg l^{-1}
filtered Zn	Zn_{fil}	PC filter	acid washed PP bottle, +HNO_3, 4°C	ICP-MS	0.1 μg l^{-1}
not filtered Zn	Zn_{tot}	No	acid washed PP bottle, +HNO_3, 4°C	ICP-MS	0.1 μg l^{-1}
filtered Cr	Cr_{fil}	PC filter	acid washed PP bottle, +HNO_3, 4°C	ICP-MS	0.1 μg l^{-1}
not filtered Cr	Cr_{tot}	No	acid washed PP bottle, +HNO_3, 4°C	ICP-MS	0.1 μg l^{-1}
filtered Ni	Ni_{fil}	PC filter	acid washed PP bottle, +HNO_3, 4°C	ICP-MS	0.1 μg l^{-1}
not filtered Ni	Ni_{tot}	No	acid washed PP bottle, +HNO_3, 4°C	ICP-MS	0.1 μg l^{-1}
filtered Fe	Fe_{fil}	PC filter	acid washed PP bottle, +HNO_3, 4°C	ICP-MS	1.0 μg l^{-1}
not filtered Fe	Fe_{tot}	No	acid washed PP bottle, +HNO_3, 4°C	ICP-MS	1.0 μg l^{-1}

4.4 Data handling

Monthly and annual mean concentrations in precipitation were calculated by weighting weekly concentrations with the corresponding sampled precipitation volume. Monthly and annual wet depositions were then determined by multiplying these mean concentrations by the precipitation volume recorded at a nearby meteorological station. This approach was chosen to minimize of underestimating monthly and annual depositions due to occasional gaps in weekly sampling.

For the sampling sites, precipitation data from the pluviometric stations operated by MeteoSwiss (ACQ → Comprovasco, LOC → Locarno Monti, LUG → Lugano, ROB → Robiei, STA → Stabio) and Canton Ticino (BIG → Cavergno, SON → Sonogno) were used.

Between 2015 and 2022, NO_3 concentrations and depositions at ROB were occasionally affected by the emission of a generator. To correct for this local contamination, nitrate concentrations were estimated using data from the nearby Italian sampling site Devero (DEV), located 23 km away. Monthly and annual mean concentrations in rainwater at DEV were provided by the Institute of Ecosystem Study (Verbania Pallanza, Italy).

At ROB, elevated NO_3 concentrations also affected total alkalinity (TAlk) and pH values. To approximate TAlk concentrations in the absence of local pollution, values were approximated using ANC (=$Ca+Mg+Na+K+ NH_4-SO_4-NO_3-Cl$), whereas pH values could not be reliably reconstructed. Total acidifying deposition was calculated subtracting the deposition of ANC from twice the deposition of NH_4 ($SO_4+NO_3+Cl+NH_4- Ca-Mg-Na-K$).

4.5 Statistical methods used for trend analysis

Trend analyses were performed using the Mann-Kendall test to identify temporal trends in wet deposition as well as in lake and in river water chemistry. For wet deposition, a seasonal Mann-Kendall test (SKT, Hirsch et al. 1982) was applied to monthly mean concentrations and depositions. For river water chemistry, a partial SKT was performed on monthly measurements, using discharge as a covariate to account for flow variability. For both wet deposition and river chemistry a correction among block was considered (Hirsch and Slack 1984). For lake chemistry a simple Mann-Kendall test (KT) (Mann 1945) was applied to autumn concentrations. In all cases, the two sided tests for the null hypothesis of no trend were rejected if p-values were below 0.05.

Temporal variations in wet deposition, river, and lake water chemistry were quantified using the Sen's slope estimator (Gilbert 1987). All trend analyses were carried out with the CRAN package "rkt 1.4" (Marchetto 2015).

4.6 Wet deposition

4.6.1 Spatial variations

Tab. 4.2 presents the annual mean concentrations of key chemical parameters in rainwater, along with their yearly depositions for 2023 and 2024.

Table 4.2 Yearly mean rainwater concentrations and depositions in 2023 and 2024.

Sampling site	Year	Precipitation MeteoCH (mm)	Analysed precipitation (mm)	Cond 25°C (µS cm⁻¹)	pH	Ca		Mg		Na		K		NH_4		HCO_3		SO_4		NO_3		Cl		TAlk	Total acidifying deposition
						Concentration (meq m⁻³)	Deposition (meq m⁻²)	Concentration (meq m⁻³)	Deposition (meq m⁻²)	Concentration (meq m⁻³)	Deposition (meq m⁻²)	Concentration (meq m⁻³)	Deposition (meq m⁻²)	Concentration (meq m⁻³)	Deposition (meq m⁻²)	Concentration (meq m⁻³)	Deposition (meq m⁻²)	Concentration (meq m⁻³)	Deposition (meq m⁻²)	Concentration (meq m⁻³)	Deposition (meq m⁻²)	Concentration (meq m⁻³)	Deposition (meq m⁻²)	Concentration (meq m⁻³)	Deposition (meq m⁻²)
ACQ	2023	1187	1104	5	6.0	9	10	2	2	4	5	1	1	25	29	17	21	7	8	11	13	4	5	17	37
	2024	1303	1081	9	5.9	46	20	4	5	4	5	1	2	23	30	55	71	9	12	12	15	4	5	54	-9
BIG	2023	1429	1326	8	6.0	25	36	4	4	5	8	3	4	30	43	34	49	9	13	16	23	6	8	34	36
	2024	2011	1739	12	5.9	59	119	3	9	5	11	2	5	29	59	67	134	14	28	16	33	6	12	66	-12
LOC	2023	1808	1422	9	6.1	12	22	3	5	8	14	1	3	47	85	31	55	11	20	21	38	7	13	30	114
	2024	1849	1581	12	6.0	55	102	5	9	7	13	1	3	30	55	64	119	13	24	16	29	7	12	64	-7
LUG	2023	1255	1255	9	6.2	10	15	2	3	5	8	2	3	48	71	32	46	11	16	20	30	6	9	32	97
	2024	1565	1566	8	6.0	23	41	4	6	5	10	2	3	32	57	37	65	10	18	15	27	6	11	36	53
ROB	2023	2051	1455	5	5.7	10	22	2	3	2	5	1	2	20	40	13	27	7	14	13	27	3	6	12	56
	2024	2650	2231	8	5.6	34	90	3	8	3	7	1	3	16	44	29	76	9	24	18	48	3	8	27	16
SON	2023	2201	1343	5	6.0	8	18	1	3	4	8	1	3	24	54	17	37	7	15	11	25	4	9	17	69
	2024	2120	1605	9	6.0	41	87	3	7	4	8	1	3	27	58	53	111	9	19	12	26	4	8	52	7
STA	2023	1364	1218	11	6.1	12	16	3	4	7	10	2	3	58	79	38	52	12	16	23	32	8	11	38	104
	2024	2279	1749	9	6.1	21	47	3	7	7	15	2	4	38	87	37	84	11	24	17	39	6	14	37	91

In general, ion concentrations of anthropogenic origin (SO_4, NO_3, NH_4) continue to decrease with increasing latitude and altitude, although these gradients are less pronounced compared to the early years of monitoring. In both 2023 and 2024, the highest concentrations of the combined SO_4, NO_3 and NH_4 were observed at STA, while the lowest were recorded at ROB. This spatial pattern reflects the influence of long-range transboundary air pollution moving along a south to north gradient from the Po plain toward the Alps and the distance from pollution sources.

The wet deposition of atmospheric pollutants is determined by their concentrations and the amount of precipitation. Typically, the highest precipitation occurs in the north-western part of Canton Ticino due to humid air masses predominantly moving from the southwest toward the Alps. The region's distinctive orography forces these air masses to rise rapidly, resulting in increased precipitation at higher altitudes.

Over the past two years, the highest deposition rates of the combined SO_4, NO_3 and NH_4 were observed at LOC in 2023 and at STA in 2024, while the lowest values were consistently recorded at ACQ. Similarly, total acidifying deposition peaked at LOC in 2023 and at STA in 2024, while the lowest values observed at ACQ and BIG in both years.

4.6.2 Seasonal variations

Fig. 4.1 shows the monthly mean concentrations of key parameters during 2023 and 2024 (on the right) and the monthly mean concentrations during 2001-2020 (on the left).

The monthly concentrations of SO_4 typically peak in summer and are lowest in winter. This pattern reflects the oxidation rate of SO_2 to SO_4, which is highest in summer and lowest in winter. At high altitudes, this is also influenced by seasonal thermal convection, with vertical transport often absent during the winter months.

The monthly mean concentrations of NO_3 are generally highest in March and lowest in November and December. The peak in NO_3 at the end of winter is likely due to a combination of high NO_2 concentrations in winter, increased oxidation rates of NOx to NO_3 in spring (which are lowest in winter and highest in summer), and the lack of vertical pollutant transport during the winter, especially at higher altitudes, due to reduced thermal convection.

The seasonal variations in NH_4 concentrations mirror those of SO_4. Hedin et al. (1990) explained this similarity through a chemical coupling between NH_4 and SO_4, with acidic SO_4 aerosols facilitating the long-range transport of NH_4. Therefore, seasonal changes in NH_4 concentrations at locations far from major NH_4 emission sources can be strongly influenced by the availability of SO_4 aerosols and seasonal variations in the emissions and oxidation of SO_2.

Concentrations of Ca^{2+} + Mg^{2+} + K^+ are typically highest in late spring and autumn, and lowest in winter. The reduced concentrations during winter may be linked to atmospheric

temperature inversions that limit the vertical transport of dust to higher altitudes. The higher concentrations in spring and autumn are likely associated with more frequent Saharan dust events, which tend to peak between March and June, and again in October and November (https://www.meteoswiss.admin.ch/weather/weather-and-climate-from-a-to-z/saharan-dust.html).

Concentrations of Cl and Na are generally low and similar, because of the common sea salt source.

When compared the averages for 2001-2020 to those for 2023 and 2024, concentrations of SO_4 and NO_3 remained consistent. Differently, concentrations of NH_4 were slightly higher in 2023 and similar in 2024. The higher NH_4 concentrations observed, especially in summer 2023 and already in summer 2022, may be linked to increased ammonia evaporation from agriculture, driven by higher-than-average temperatures combined with low precipitation.

Both TAlk and pH were higher in 2023 and 2024 compared to the 2001-2020 average. Specifically, only 2% of the rainwater samples collected in 2023 and 2024 had pH values below 5, compared to 18% in the 2001-2020 period. Furthermore, 40% of the 2023 and 2024 samples had pH values between 5.5 and 6, and 58% had pH values above 6.0. In contrast, during the 2001-2020 period, 50% of samples had pH values between 5.5 and 6, and 31% had pH values above 6.0.

Single concentration peaks are often associated with low precipitation volumes, as seen in the February 2023 concentration spikes. The increases in base cations and TAlk in March, April and June 2024 were caused by Saharan dust events (MeteoSwiss 2025). These events also contributed to the significantly higher annual mean concentrations of Ca, Mg, and TAlk, as well as the notably lower total acidifying deposition in 2024 compared to 2023 (Tab. 4.2).

The monthly variations in wet depositions generally mirror the patterns of concentrations, with the difference that the amount of precipitation gains further importance (Fig. 4.3). Average (2001-2020) monthly depositions of SO_4, NO_3, NH_4, Ca+Mg+K+Na and the total acidifying deposition are normally higher during the warm months when both concentrations and precipitations are higher.

Figure 4.1 Monthly mean concentrations of key parameters in precipitation during 2023-2024 (left) during 2001-2020 (right)

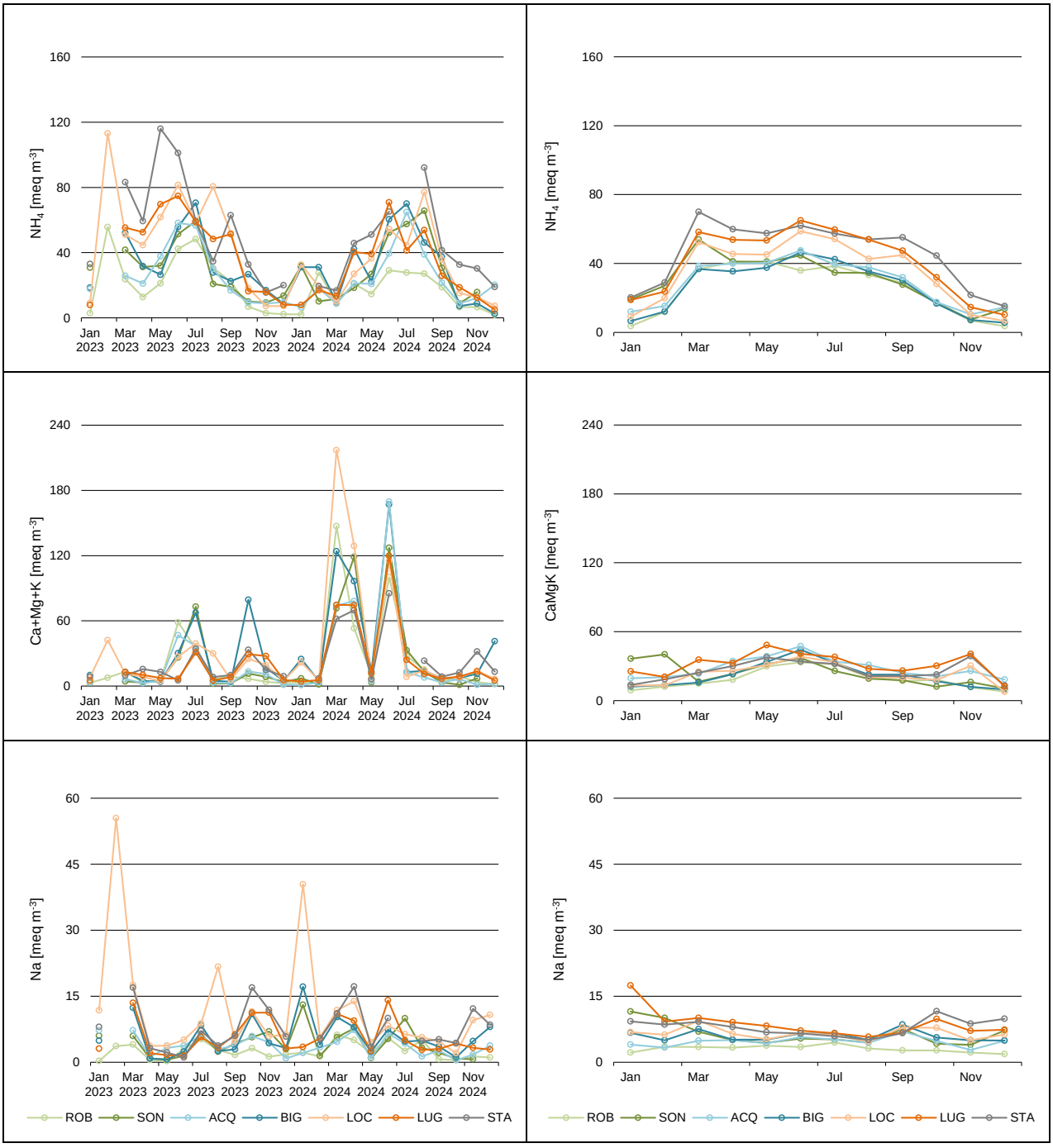
NH4 [meq m-3]
Ca+Mg+K [meq m-3]
CaMgK [meq m-3]
Na [meq m-3]
Jan 2023
Mar 2023
May 2023
Jul 2023
Sep 2023
Nov 2023
Jan 2024
Mar 2024
May 2024
Jul 2024
Sep 2024
Nov 2024
Jan
Mar
May
Jul
Sep
Nov
ROB
SON
ACQ
BIG
LOC
LUG
STA

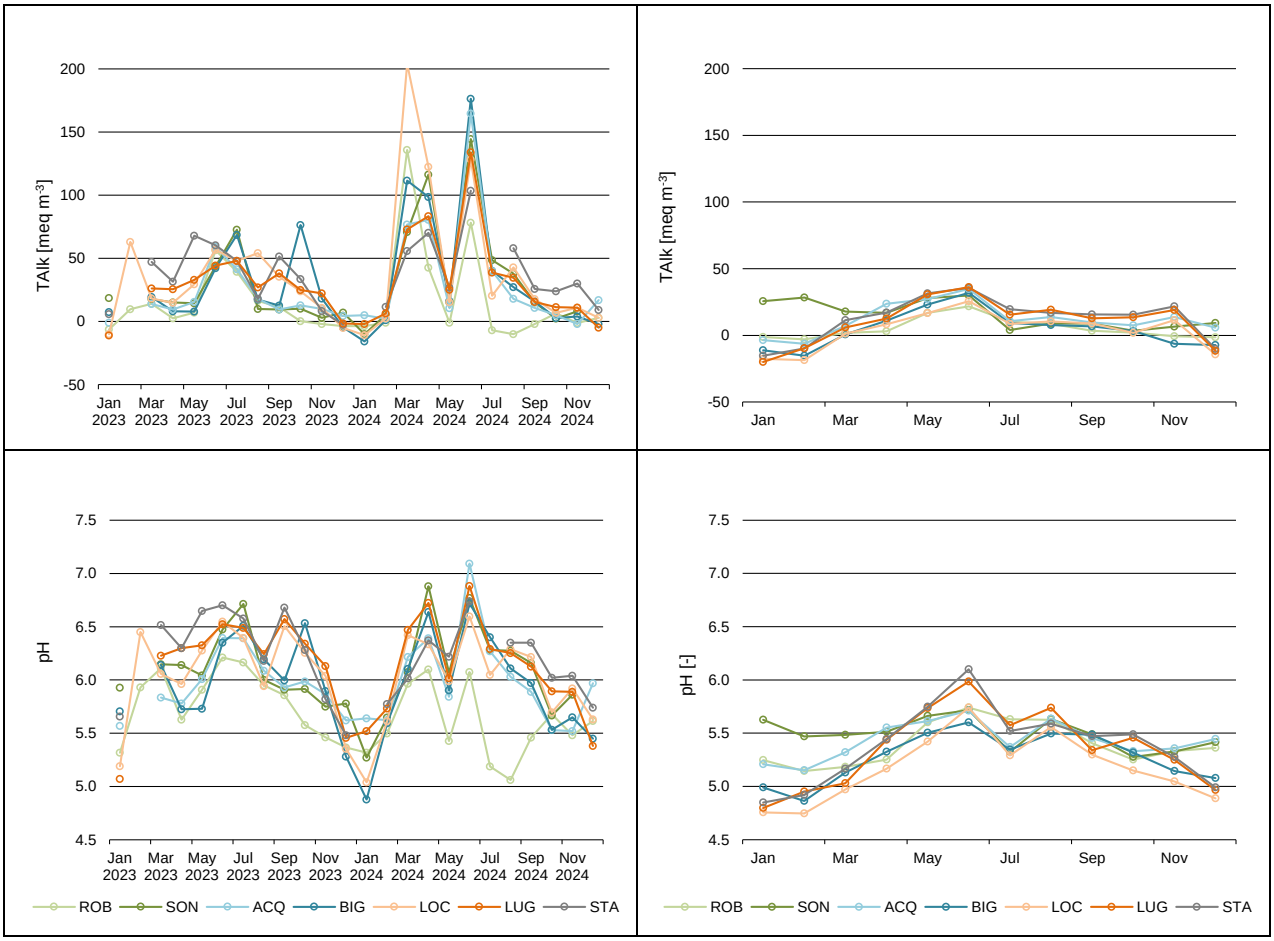
TAlk [meq m-3]
200
150
100
50
0
-50
Jan 2023
Mar 2023
May 2023
Jul 2023
Sep 2023
Nov 2023
Jan 2024
Mar 2024
May 2024
Jul 2024
Sep 2024
Nov 2024
Jan
Mar
May
Jul
Sep
Nov
pH
pH [-]
7.5
7.0
6.5
6.0
5.5
5.0
4.5
ROB
SON
ACQ
BIG
LOC
LUG
STA

Figure 4.2 Monthly mean depositions of key parameters in precipitation during 2023-2024 (left) during 2001-2020 (right)

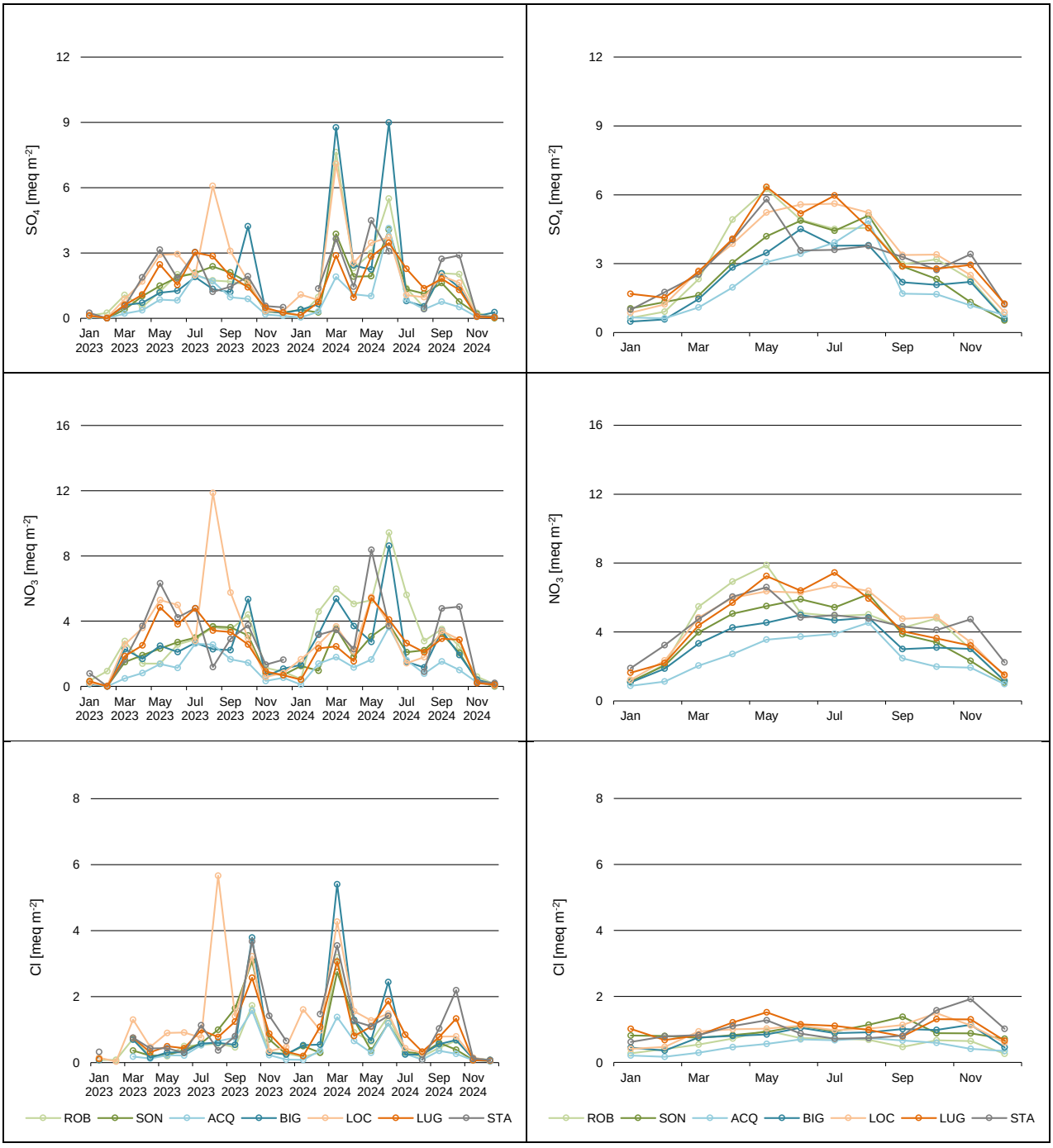

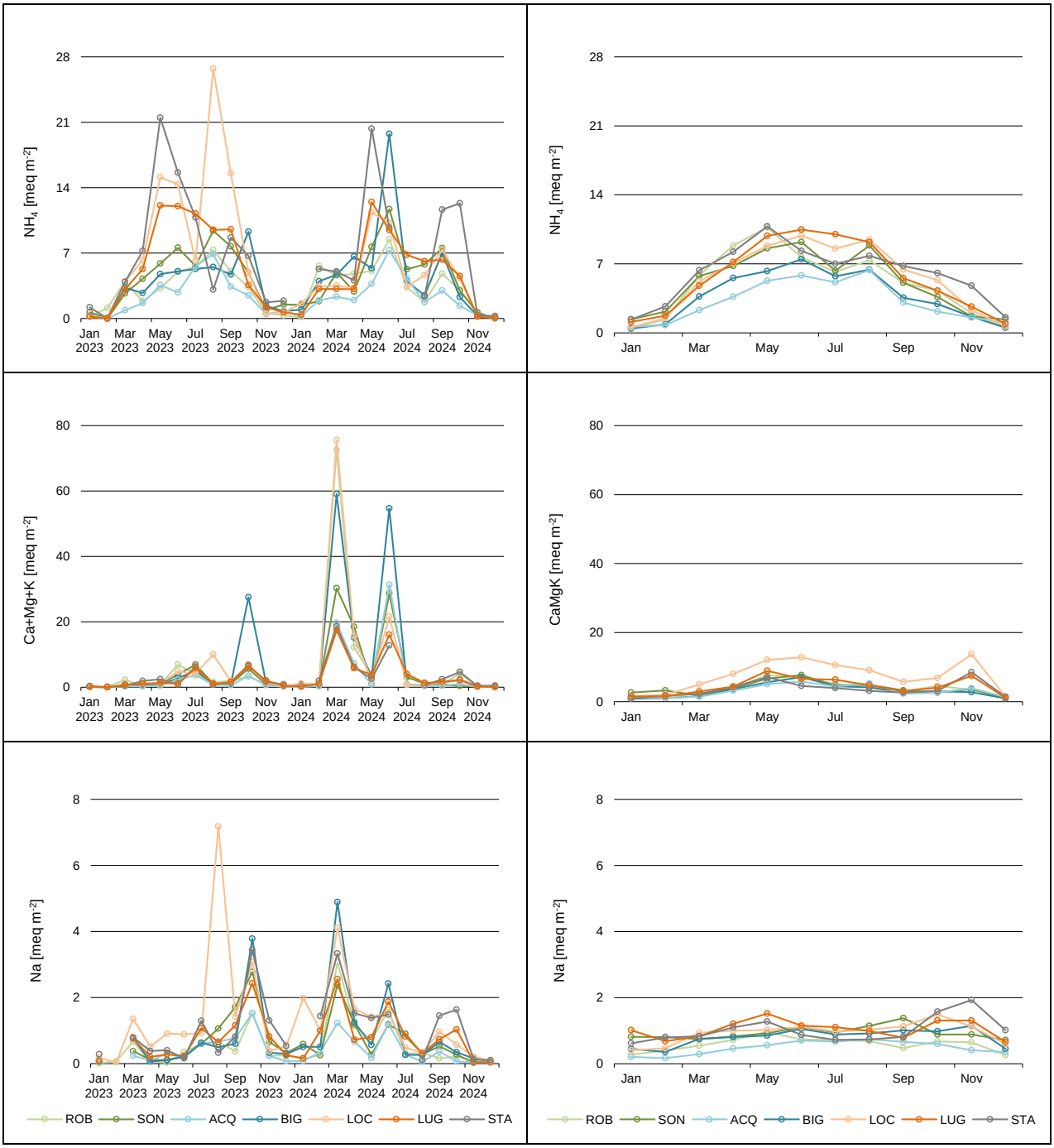
NH4 [meq m-2]
28
21
14
7
0
Jan 2023
Mar 2023
May 2023
Jul 2023
Sep 2023
Nov 2023
Jan 2024
Mar 2024
May 2024
Jul 2024
Sep 2024
Nov 2024
Jan
Mar
May
Jul
Sep
Nov
Ca+Mg+K [meq m-2]
80
60
40
20
0
CaMgK [meq m-2]
Na [meq m-2]
8
6
4
2
0
ROB
SON
ACQ
BIG
LOC
LUG
STA

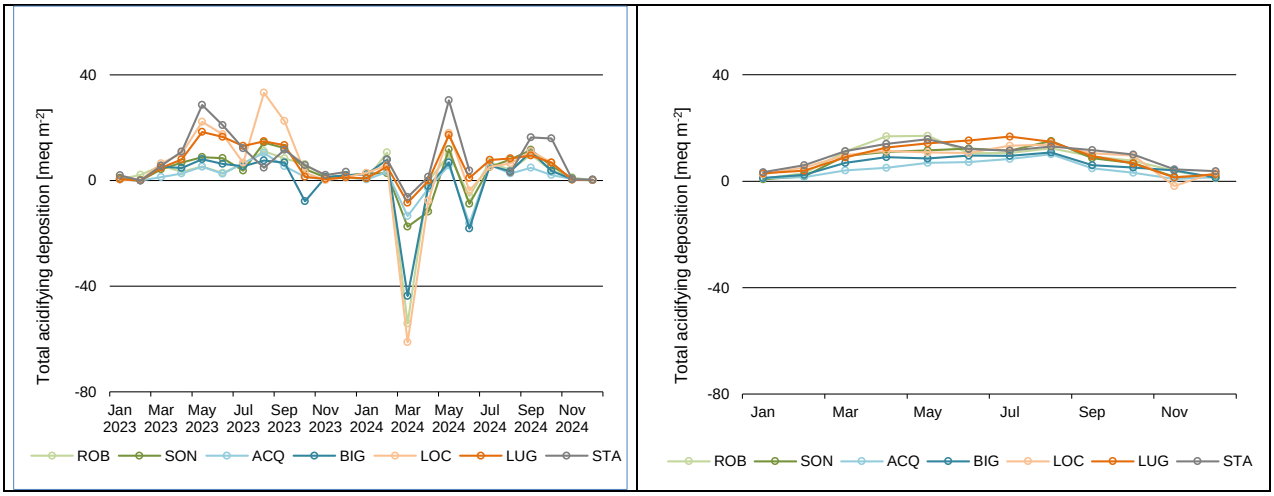
40
0
-40
-80
Total acidifying deposition [meq m-2]
Jan 2023
Mar 2023
May 2023
Jul 2023
Sep 2023
Nov 2023
Jan 2024
Mar 2024
May 2024
Jul 2024
Sep 2024
Nov 2024
ROB
SON
ACQ
BIG
LOC
LUG
STA
Jan
Mar
May
Jul
Sep
Nov

4.6.3 Temporal variations

Fig. 4.3 presents the annual mean concentrations and depositions of the key parameters from the 1980's to 2024, while Tab. 4.3 provides the Sen's slopes and the significance of the temporal trends. Trends analyses were conducted for three distinct time periods: from the beginning of measurements to 2024, from the start of measurements to 2010, and from 2010 until 2024. Since deposition trends can be significantly affected by irregular fluctuations in precipitation volumes, trend analyses for depositions were only performed for the entire monitoring period to minimize the influence of varying rainfall.

As a direct consequence of the reduced SO_2 emissions, concentrations and depositions of SO_4 decreased sharply after 1990. This decline was significant at all sites, with the steepest reductions observed at the most polluted locations (LOC, LUG, and STA) during the period from 1988–1991 to 2015. Although SO_4 concentrations continued to decrease significantly at all sites after 2015, the rate of decline was notably slower.

Similarly, reduced NO_x emissions led to a significant decrease in NO_3 concentrations and depositions at all sites, with the most pronounced reductions occurring between 2000 and 2015.

Concentrations and depositions of NH_4 also showed a slight but statistically significant decrease at five of the seven sites). However, the unusually high NH_4 concentrations observed in 2022 and 2023 may be linked to increased ammonia evaporation from agricultural sources due to particularly warm and dry summers.

Concentrations of the sum of Ca, Mg and K significantly decreased at six out of seven sites, while depositions declined at five of the seven sites. Alkaline rain events became less frequent until 2017, but have seemingly increased since then. According to Mark Parrington, Senior Scientist at the Copernicus Atmosphere Monitoring Service (CAMS), the intensity and frequency of these episodes have risen in recent years, possibly due to changes in atmospheric circulation patterns (https://atmosphere.copernicus.eu/new-exceptionally-intense-saharan-dust-episode-through-western-europe).

Na and Cl concentrations and depositions also significantly declined at most sites, particularly between the 1990s and 2000. Frequent sea salt episodes caused by Atlantic storms have been reported in coastal areas in Northern European countries (Wright and

Jenkins 2001), and it is possible these events had a minor influence on the rain quality in Switzerland. However, measures to reduce sulfur emissions also resulted in reduced HCl emissions from combustion processes (Evans et al., 2011) and the strong correlation between Na and Cl suggests that sea salt was the primary source of elevated concentrations in the early 1990s.

Concentrations of the hydrogen ions (H) and TAlk showed significant changes, with H concentrations decreasing and TAlk increasing at all sites. The most pronounced changes occurred before 2010, but trends remained significant thereafter. TAlk concentrations rose from around -40 to and -30 meq m^{-3} to approximately 30-40 meq m^{-3}, except at ROB, where the mean TAlk over the last five years was 17 meq m^{-3}. Similarly, mean pH values increased from around 4.3 in the 1990s to approximately 6.0, except at ROB, which recorded a mean pH of 5.5 over the last five years..

The concentration peaks of SO_4 and base cations (Ca+Mg+K, Na) at LUG in 2010 were the consequence of the volcanic eruption at Eyafjellajokull (Iceland) in April 2010.

Figure 4.3 Annual mean concentrations (left), depositions (right) of key parameters in precipitation.


NH4 [meq m-3]
NH4 [meq m-2]
Ca+Mg+K [meq m-3]
Ca+Mg+K [meq m-2]
Na [meq m-3]
Na [meq m-3]
ROB
SON
ACQ
BIG
LOC
LUG
STA

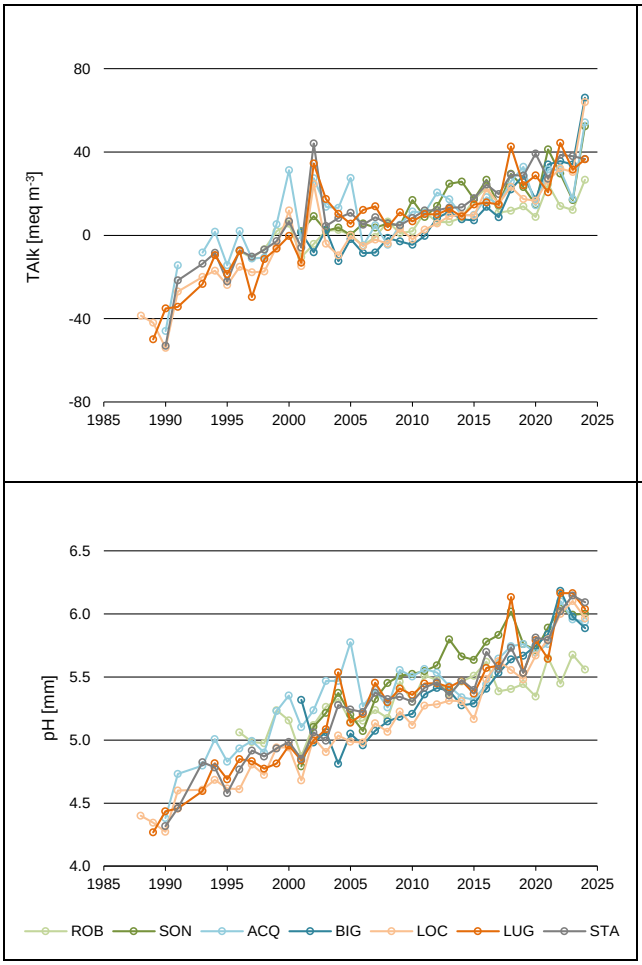
TAlk [meq m-3]
80
40
0
-40
-80
1985
1990
1995
2000
2005
2010
2015
2020
2025

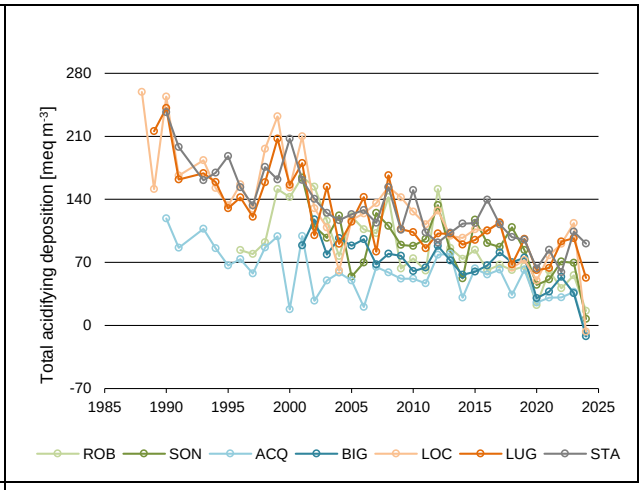
Total acidifying deposition [meq m-3]
280
210
140
70
0
-70
1985
1990
1995
2000
2005
2010
2015
2020
2025
ROB
SON
ACQ
BIG
LOC
LUG
STA

pH [mm]
6.5
6.0
5.5
5.0
4.5
4.0
1985
1990
1995
2000
2005
2010
2015
2020
2025
ROB
SON
ACQ
BIG
LOC
LUG
STA

Table 4.3 Sen's slopes of concentrations (in meq m^{-3} yr^{-1}) and depositions (in meq m^{-2} yr^{-1}) of key parameters in precipitation. Red rates indicate significant trends

CONC (meq m^{-3} yr^{-1})	Period	SO_4 beginning-2024	NO_3 beginning-2024	Cl beginning-2024	NH_4 beginning-2024	Ca+Mg+K beginning-2024	Na beginning-2024	H beginning-2024	TAlk beginning-2024
ACQ	1990-2024	-1.08	-0.62	-0.08	-0.20	-0.66	-0.12	-0.29	1.21
BIG	2001-2024	-0.57	-0.60	0.00	0.07	-0.02	-0.03	-0.37	1.67
LOC	1988-2024	-1.55	-0.86	-0.13	-0.35	-0.42	-0.08	-0.86	2.10
LUG	1989-2024	-1.71	-0.90	-0.16	-0.39	-0.70	-0.19	-0.53	1.83
ROB	1996-2024	-0.54	-0.33	0.00	-0.21	-0.14	-0.03	-0.26	0.74
SON	2001-2024	-0.56	-0.54	-0.04	-0.02	-0.24	-0.09	-0.17	1.13
STA	1990-2024	-1.69	-0.85	-0.11	-0.29	-0.53	-0.11	-0.44	1.98

CONC (meq m^{-3} yr^{-1})	Period	SO_4		NO_3		Cl		NH_4		Ca+Mg+K		Na		H		TAlk	
		beginning-2010	2010-2024	beginning-2010	2010-2024	beginning-2010	2010-2024	beginning-2010	2010-2024	beginning-2010	2010-2024	beginning-2010	2010-2024	beginning-2010	2010-2024	beginning-2010	2010-2024
ACQ	1990-2024	-1.14	-0.68	-0.52	-0.86	0.00	0.01	-0.43	-0.15	0.06	-0.82	-0.21	0.02	-0.82	-0.14	1.83	1.08
BIG	2001-2024	-1.27	-0.33	-1.19	-0.56	0.15	0.08	-1.20	0.35	-0.44	0.20	0.15	0.10	-0.56	-0.23	0.42	1.86
LOC	1988-2024	-2.40	-0.64	-0.71	-1.18	-0.43	0.17	-0.53	0.06	-0.62	-0.18	-0.31	0.23	2.56	-0.23	2.56	1.94
LUG	1989-2024	-1.93	-0.76	-0.36	-0.87	-0.25	0.03	-0.12	0.22	-0.13	-0.28	-0.17	-0.06	-1.37	-0.11	2.75	1.33
ROB	1996-2024	-0.77	-0.26	0.07	-0.32	-0.02	0.05	-0.11	-0.14	-0.24	-0.09	-0.13	0.04	-0.33	-0.10	0.52	0.44
SON	2001-2024	-1.14	-0.45	-0.66	-0.73	-0.12	-0.08	-0.88	-0.15	-0.65	-0.45	-0.35	-0.12	-0.42	-0.08	0.57	0.72
STA	1990-2024	-2.57	-0.58	-0.90	-0.64	-0.31	0.08	-0.46	0.60	-1.23	0.15	-0.21	0.08	-1.06	-0.08	2.39	1.94

DEP (meq m^{-2} yr^{-1})	Period	SO_4 beginning-2024	NO_3 beginning-2024	Cl beginning-2024	NH_4 beginning-2024	Ca+Mg+K beginning-2024	Na beginning-2024	H beginning-2024	Total acidifying deposition beginning-2024
ACQ	1990-2024	-1.13	-0.81	-0.09	-0.27	-0.63	-0.10	-0.35	-1.40
BIG	2001-2024	-0.58	-0.67	0.00	0.01	-0.03	-0.03	-0.41	-2.25
LOC	1988-2024	-2.06	-1.27	-0.17	-0.51	-0.48	-0.11	-1.24	-3.47
LUG	1989-2024	-2.20	-1.18	-0.18	-0.41	-0.81	-0.21	-0.76	-2.96
ROB	1996-2024	-1.09	-0.81	-0.01	-0.37	-0.20	-0.05	-0.53	-2.19
SON	2001-2024	-0.94	-1.22	-0.12	-0.39	-0.48	-0.21	-0.30	-2.05
STA	1990-2024	-2.08	-1.24	-0.16	-0.41	-0.67	-0.15	-0.60	-2.91

4.7 Alpine lakes

4.7.1 Introduction

Over the past two years, lake sampling was carried out on 25 September 2023, 6 November 2023, 24 September 2024, and 21 October 2024. Fig. 4.4 shows the daily precipitation volumes recorded at ROB during the sampling periods. With the exception of the first sampling in 2024, each sampling date were preceded by several consecutive days of rainfall.

Figure 4.4 Daily precipitation at ROB during the sampling months in 2023 and 2024. Sampling dates are indicated with red bars.

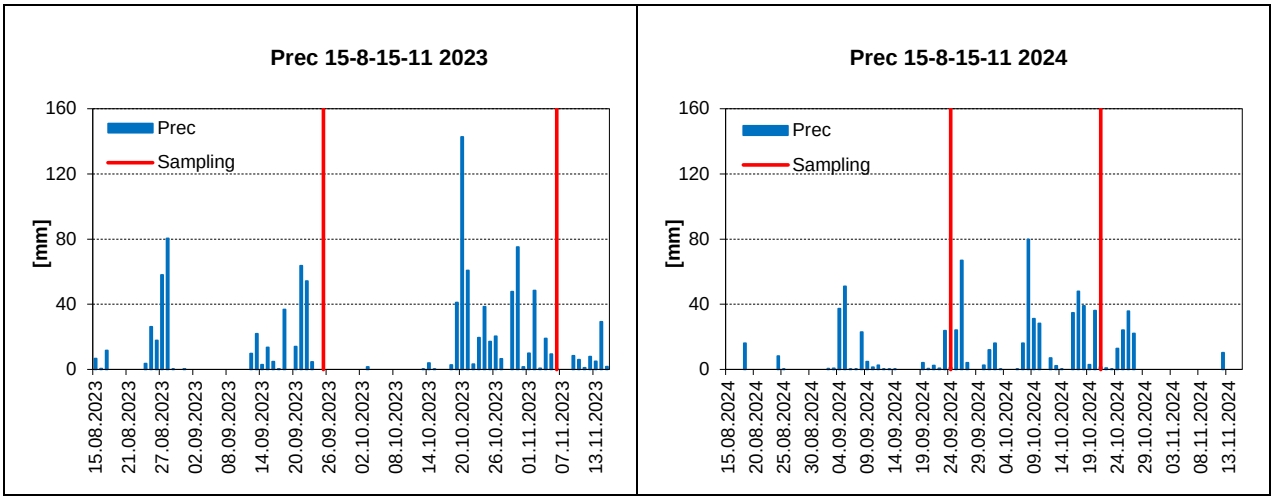

4.7.2 Autumn mean concentrations of key parameters in lake surface waters

Table 4.4 presents the average autumn concentrations of key chemical parameters measured in lake surface waters in 2023 and 2024.

In 2023 and Cond at 25°C ranged from 6 and 32 µS cm^{-1}, pH from 5.4 to 7.1, TAlk from -4 to 99 meq m^{-3}. The sum of base cations (Ca, Mg, Na, K) varied between 38 and 253 meq m^{-3}, SO_4 between 10 and 221 meq m^{-3}, NO_3 between 4 and 26 meq m^{-3} and TN between 0.2 and 0.6 mg N l^{-1}. SiO_2 concentrations ranged from 1.2 and 3.2 mg SiO_2 l^{-1}, Al_{sol} from 4 to 268 µg l^{-1}, and DOC between 0.3 and 1.3 mg C l^{-1},

The concentrations of Pb_{sol} and Ni_{sol} remained below the European surface water quality standards for annual means (Pb_{sol}: 7.2 µg l^{-1}, Ni_{sol}: 20 µg l^{-1}; Directive 2008/105/EC). However, RAl exceeded US EPA chronic critical values in STA in 2023 (~47 µg l^{-1}) and in GAR in both 2023 and 2024 (~8 µg l^{-1}).<

Aluminum is the third most abundant element in the Earth's crust, commonly found in soils and rocks. In high-altitude lakes, weathering is the primary source of aluminum. Elevated aluminum levels can disrupt ion regulation and impair respiratory functions in aquatic species. While aquatic plants are generally less sensitive, fish and other aquatic organisms can be significantly affected.

The bioavailability of aluminum, and consequently its potential toxicity, depends on water chemistry, particularly pH, total hardness, and DOC. Low pH, low DOC, and low water hardness increase aluminum solubility and toxicity. In sensitive aquatic ecosystems, high aluminum concentrations can compromise the survival of fish and invertebrates, highlighting the importance of monitoring these key parameters.

Table 4.4 Autumn mean concentrations of the parameters measured lakes surface water during 2023 and 2024 and chronic and acute critical freshwater levels for Al_{tot}. Values below the quantification limit were preceded with <.

Parameter	Year	STA	TOM	POR	BAR	GAR	LEI	MOR	MOG	INF	SUP	NER	FRO	ANT	CRO	ORS	SCH	POZ	SFI	SAS	ALZ
Temp (°C)	2023	6	7	4	7	8	8	5	6	7	7	7	5	7	7	8	6	6	8	6	9
	2024	9	8	4	5	6	6	6	7	6	6	5	5	6	8	4	5	8	8	7	9
Cond 25°C (µS cm^{-1})	2023	6.5	7.0	20.4	9.3	6.3	27.5	15.0	18.8	11.4	9.7	19.6	14.8	13.3	7.5	10.3	9.5	7.3	9.9	9.2	17.7
	2024	5.5	6.8	22.1	9.0	6.6	32.3	15.3	21.9	8.8	8.2	19.3	12.3	13.8	6.7	8.7	7.7	7.0	9.5	6.9	15.5
pH	2023	5.4	6.0	6.8	6.3	5.6	6.4	6.6	6.7	6.8	6.7	7.0	6.8	7.1	6.6	7.0	6.6	6.6	6.5	6.1	6.9
	2024	5.8	6.1	6.8	6.4	5.7	6.4	6.7	6.9	6.7	6.6	6.9	6.7	7.0	6.6	6.6	6.5	6.8	6.6	6.0	6.9
TAlk (meq m^{-3})	2023	-4	10	64	24	3	29	50	51	60	54	83	67	88	37	56	42	36	54	20	99
	2024	10	17	72	28	5	35	55	71	46	47	91	55	98	39	50	37	40	49	17	94
Ca (meq m^{-3})	2023	16	29	114	45	17	117	71	87	57	49	113	91	83	34	50	42	32	52	34	88
	2024	17	31	139	49	22	150	77	110	44	42	118	76	90	34	51	41	34	50	25	86
Mg (meq m^{-3})	2023	6	5	12	6	7	51	18	24	9	8	17	9	6	5	7	7	7	9	10	17
	2024	6	5	14	7	9	64	19	28	7	7	16	8	6	5	7	7	7	8	8	17
Na (meq m^{-3})	2023	13	14	19	13	8	21	18	24	17	14	20	15	21	15	16	13	16	20	17	24
	2024	12	13	20	11	8	23	17	28	13	11	19	10	21	12	12	10	15	18	11	21
K (meq m^{-3})	2023	5	4	14	6	6	16	15	15	12	10	15	9	9	6	6	7	5	5	10	14
	2024	4	4	14	5	6	17	15	16	10	9	16	7	9	5	5	7	5	4	7	14
NH_4 (meq m^{-3})	2023	2	1	1	1	2	2	1	1	1	1	1	1	1	2	0	0	1	1	1	2
	2024	3	1	1	1	1	1	1	1	1	1	1	1	1	1	1	1	1	1	1	2
SO_4 (meq m^{-3})	2023	17	22	85	37	30	172	61	85	28	21	74	47	14	12	14	18	15	21	21	29
	2024	16	23	106	37	35	221	67	100	22	18	74	39	15	10	13	16	15	22	18	30
NO_3 (meq m^{-3})	2023	15	15	16	12	8	11	12	15	11	9	8	11	17	13	20	20	8	9	26	14
	2024	9	15	11	10	7	9	9	13	9	8	8	9	15	11	15	14	4	10	16	17
NO_2 (µg N l^{-1})	2023	0	0	0	1	1	1	1	1	0	1	1	1	1	1	2	1	0	0	1	1
	2024	1	1	1	1	1	1	1	1	1	1	0	0	2	1	1	0	0	1	0	2
Cl (meq m^{-3})	2023	6	4	3	4	2	3	4	4	3	4	4	4	4	5	3	3	5	4	6	6
	2024	5	3	3	3	2	3	3	4	3	3	3	2	4	3	3	3	4	4	4	5
SRP (µg P l^{-1})	2023	<2	<2	<2	<2	<2	<2	<2	<2	<2	<2	<2	<2	<2	<2	<2	<2	<2	<2	<2	<2
	2024	<2	<2	<2	<2	<2	<2	<2	<2	<2	<2	<2	<2	<2	<2	<2	<2	<2	<2	<2	<2
P_{tot} (µg P l^{-1})	2023	2.4	<2	3	<2	<2	11.5	4.7	4.3	2.9	3.3	2.1	3.5	2.3	2.2	3.6	2.9	2.1	2.3	2.2	3.9
	2024	4.3	3.6	6.4	6.0	2.6	5.2	4.8	5.9	4.7	6.0	5.4	5.6	4.9	4.2	6.9	7.5	6.4	4.9	6.7	4.5
N_{tot} (mg N l^{-1})	2023	0.36	0.31	0.31	0.29	0.21	0.34	0.27	0.32	0.30	0.33	0.21	0.28	0.38	0.29	0.50	0.41	0.26	0.26	0.59	0.35
	2024	0.37	0.41	0.27	0.24	0.23	0.26	0.24	0.28	0.25	0.27	0.23	0.21	0.36	0.38	0.34	0.45	0.30	0.28	0.35	0.38
DOC (mg C l^{-1})	2023	1.1	0.5	0.3	0.4	0.4	0.5	0.4	0.5	0.6	0.6	0.3	0.4	0.4	0.4	0.7	0.4	1.0	0.8	0.9	0.7
	2024	1.3	0.6	0.4	0.3	0.3	0.4	0.4	0.4	0.5	0.6	0.3	0.4	0.4	0.4	0.4	0.5	1.2	0.8	1.0	0.6
SiO_2 (mg l^{-1})	2023	2.0	2.1	3.0	1.7	1.2	2.0	2.2	2.9	2.1	1.8	2.2	1.8	2.6	1.6	2.0	2.2	2.7	2.7	2.6	3.2
	2024	1.7	1.9	2.9	1.7	1.0	2.4	2.2	3.2	1.6	1.5	2.1	1.4	2.8	1.6	1.9	1.9	2.5	2.3	2.2	2.9

Parameter	Year	STA	TOM	POR	BAR	GAR	LEI	MOR	MOG	INF	SUP	NER	FRO	ANT	CRO	ORS	SCH	POZ	SFI	SAS	ALZ
RAl (µg l^{-1})	2023	54.0	19.9	4.2	4.5	17.6	17.7	8.8	7.7	6.5	7.2	2.7	5.7	5.3	2.7	8.1	8.6	21.5	22.0	29.3	10.1
	2024	41.5	13.5	3.6	3.0	11.9	6.0	5.6	10.8	6.3	9.1	2.9	6.7	8.2	3.3	5.4	9.7	30.5	16.8	34.1	10.2
Al_{tot} (µg l^{-1})	2023	64.9	26.4	6.3	7.5	20.5	267.6	129.3	38.1	12.9	15.2	4.4	11.2	8.8	4.9	18.1	13.6	27.5	27.5	35.1	13.0
	2024	64.6	22.4	8.4	11.2	18.2	26.6	22.3	18.1	17.8	17.2	4.9	11.4	11.4	7.3	18.1	12.8	38.8	26.9	39.2	15.3
Pb_{sol} (µg l^{-1})	2023	0.4	<0.1	<0.1	<0.1	<0.1	<0.1	<0.1	<0.1	<0.1	<0.1	<0.1	<0.1	<0.1	<0.1	<0.1	<0.1	<0.1	<0.1	<0.1	<0.1
	2024	<0.1	<0.1	<0.1	<0.1	<0.1	<0.1	<0.1	<0.1	<0.1	<0.1	<0.1	<0.1	<0.1	<0.1	<0.1	<0.1	<0.1	<0.1	<0.1	<0.1
Pb_{tot} (µg l^{-1})	2023	0.3	0.2	<0.1	<0.2	<0.1	0.3	0.4	0.3	0.2	0.2	<0.2	<0.2	<0.1	<0.2	<0.1	<0.1	0.2	<0.2	0.3	0.2
	2024	0.1	0.2	<0.1	<0.1	<0.1	0.1	0.1	<0.1	<0.1	<0.1	<0.1	<0.1	<0.1	<0.1	<0.1	<0.1	0.1	<0.1	<0.1	<0.1
Cd_{sol} (µg l^{-1})	2023	<0.1	<0.1	<0.1	<0.1	<0.1	<0.1	<0.1	<0.1	<0.1	<0.1	<0.1	<0.1	<0.1	<0.1	<0.1	<0.1	<0.1	<0.1	<0.1	<0.1
	2024	<0.1	<0.1	<0.1	<0.1	<0.1	<0.1	<0.1	<0.1	<0.1	<0.1	<0.1	<0.1	<0.1	<0.1	<0.1	<0.1	<0.1	<0.1	<0.1	<0.1
Cd_{tot} (µg l^{-1})	2023	<0.1	<0.1	<0.1	<0.1	<0.1	<0.1	<0.1	<0.1	<0.1	<0.1	<0.1	<0.1	<0.1	<0.1	<0.1	<0.1	<0.1	<0.1	<0.1	<0.1
	2024	<0.1	<0.1	<0.1	<0.1	<0.1	<0.1	<0.1	<0.1	<0.1	<0.1	<0.1	<0.1	<0.1	<0.1	<0.1	<0.1	<0.1	<0.1	<0.1	<0.1
Cu_{sol} (µg l^{-1})	2023	0.4	0.3	0.2	0.2	0.3	0.7	0.6	0.5	0.2	0.2	0.2	0.2	0.1	0.2	0.1	0.1	0.2	0.2	0.3	0.2
	2024	0.2	0.2	0.1	0.1	0.2	0.4	0.3	0.3	0.2	0.1	0.1	0.1	0.2	0.1	0.1	0.1	0.1	0.1	0.1	0.1
Cu_{tot} (µg l^{-1})	2023	0.5	0.3	0.3	0.2	0.4	1.3	1.0	0.7	0.3	0.3	0.3	0.3	0.2	0.2	0.2	0.2	0.2	0.2	0.4	0.3
	2024	0.3	0.3	0.1	0.1	0.2	0.5	0.4	0.4	0.2	0.2	0.1	0.1	0.1	0.1	0.1	0.1	0.1	0.1	0.1	0.1
Zn_{sol} (µg l^{-1})	2023	2.7	1.5	0.3	1.3	1.0	1.1	0.9	1.2	0.6	1.0	0.6	0.7	0.4	0.5	0.5	0.2	1.3	0.8	2.0	0.9
	2024	1.6	1.2	0.1	0.2	0.9	0.9	0.5	0.4	0.8	0.4	0.1	0.1	0.3	0.5	0.2	0.2	0.2	0.7	0.8	0.2
Zn_{tot} (µg l^{-1})	2023	3.1	1.8	0.4	1.4	1.1	1.8	1.4	1.5	0.7	1.0	0.5	0.8	0.5	0.5	0.5	0.7	1.5	1.0	2.1	1.1
	2024	1.7	1.8	0.4	0.4	1.2	1.5	1.0	0.6	1.2	1.0	0.3	0.4	0.6	0.6	0.4	0.4	0.6	0.8	0.8	0.4
Cr_{sol} (µg l^{-1})	2023	<0.1	<0.1	<0.1	<0.1	<0.1	<0.1	<0.1	<0.1	<0.1	<0.1	<0.1	<0.1	<0.1	<0.1	<0.1	<0.1	<0.2	<0.1	<0.3	<0.2
	2024	<0.1	<0.1	<0.1	<0.1	<0.1	<0.1	<0.1	<0.1	<0.1	<0.1	<0.1	<0.1	<0.1	<0.1	<0.1	<0.1	<0.1	<0.1	<0.1	<0.1
Cr_{tot} (µg l^{-1})	2023	<0.1	<0.1	<0.1	<0.2	<0.1	<0.3	<0.3	<0.2	<0.1	<0.2	<0.1	<0.2	<0.1	<0.1	<0.1	<0.1	<0.3	<0.1	<0.3	<0.2
	2024	<0.1	<0.1	<0.1	<0.1	<0.1	<0.1	<0.1	<0.1	<0.1	<0.1	<0.1	<0.1	<0.1	<0.1	<0.1	<0.1	<0.1	<0.1	<0.1	<0.1
Ni_{sol} (µg l^{-1})	2023	0.2	<0.1	<0.1	0.1	1.2	8.1	0.6	1.1	<0.1	<0.1	0.2	<0.1	<0.1	<0.1	0.1	0.1	<0.1	<0.1	0.2	<0.1
	2024	0.2	0.2	0.1	0.1	1.3	10.8	0.5	0.9	0.2	0.1	0.2	0.1	0.1	0.1	0.1	0.1	0.1	0.1	0.2	0.1
Ni_{tot} (µg l^{-1})	2023	0.2	0.1	<0.1	<0.1	1.2	8.3	0.7	1.1	<0.1	<0.1	0.2	<0.1	<0.1	<0.1	<0.1	<0.1	<0.1	<0.1	0.2	<0.1
	2024	0.2	0.2	<0.1	0.1	1.3	10.7	0.5	0.9	<0.2	<0.1	0.2	0.1	<0.1	<0.1	0.1	<0.1	<0.1	<0.1	0.2	<0.1
Fe_{sol} (µg l^{-1})	2023	10.9	1.6	1.1	1.6	5.8	13.7	6.6	7.0	1.7	3.2	<1.3	<1.4	<1.0	<1.0	1.4	1.4	2.9	4.6	5.0	3.0
	2024	12.9	<1.2	<1.0	<1.0	4.5	3.8	3.3	9.5	<1.0	<3.1	2.9	1.4	<2.0	<1.0	<1.0	<1.0	<1.5	<1.5	4.9	1.2
Fe_{tot} (µg l^{-1})	2023	18.2	8.2	3.2	5.0	7.4	248.9	129.9	43.7	11.2	54.1	2.7	8.3	3.1	1.9	11.1	4.2	6.9	10.3	8.3	5.3
	2024	34.7	6.7	1.9	4.4	10.2	31.0	19.1	19.9	8.3	9.8	3.1	4.6	3.7	2.2	10.0	1.7	12.9	5.3	7.3	4.2
Al_{tot} (µg l^{-1})	chronic	47	31	78	31	8	31	78	78	78	78	180	78	180	78	78	78	110	110	47	78
	acute	70	46	130	46	13	46	130	130	130	130	300	130	300	130	130	130	190	190	70	130

4.7.3 Lake water chemistry in 2023–2024 compared to annual means of 2001-2020

Fig. 4.5 and 4.6 illustrate the primary chemical parameters measured in lake surface waters during 2023 and 2024, along their average values from 2001 to 2020.

In 2023 and 2024, the highest SO_4 concentrations were observed in lakes influenced by thawing cryospheric features, which likely enhanced sulfur weathering (e.g., POR, LEI, MOG, NER, MOR). These lakes exhibited higher SO_4 concentrations compared to 2001-2020 average. In contrast, the remaining lakes showed slightly lower SO_4 concentrations in 2023 and 2024 relative to the 2010–2020 mean.

NO_3 concentrations in 2023 and 2024 were lower than the 2001–2020 average. Variations in NO_3 concentrations between lakes are primarily driven by differences in nitrogen retention

capacity within catchments and and the transformation of inorganic nitrogen into organic forms.

Base cation concentrations are mainly controlled by weathering processes and displacement from the soil matrix, often correlated with TAlk and pH. An exception was noted in LEI, where base cation concentrations were associated with SO_4 rather than bicarbonate alkalinity. This pattern indicates the potential impact of gypsum or anhydrite, or silicate weathering coupled with sulfide oxidation. Base cation concentrations in 2023 and 2024 were similar to the long-term average from 2001–2020.

In 2023, only Lake STA exhibited TAlk values below 0 meq m^{-3}, whereas in 2024, no lakes fell below this threshold. Lakes with consistently high TAlk values (>50 meq m^{-3}) included ALZ, ANT, FRO, MOG, NER, and POR. The remaining 12 lakes displayed at least temporary sensitivity to acidification, with TAlk values between 0 and 50 meq m^{-3}. TAlk levels in 2023 and 2024 were slightly higher than the 2000–2020 averages..

pH values in 2023 and 2024 were generally consistent with the long-term average from 2001–2020..

Concentrations of RAl were highest in lakes with lower pH values. During 2001–2020, mean RAl concentrations in the most acidic lakes were 61 µg l^{-1} in STA, 38 µg l^{-1} in GAR, 25 µg l^{-1} in TOM, and 20 µg l^{-1} in SAS. In 2023 and 2024, RAl concentrations in these lakes were notably lower.

SiO_2 concentrations were generally higher in lakes with elevated base cation levels (correlation coefficients: 0.44 in 2023 and 0.62 in 2024) and higher TAlk (correlation coefficients: 0.62 in 2023 and 0.64 in 2024). This trend suggests that SiO_2 concentrations are primarily influenced by the intensity of weathering within the catchments. SiO_2 levels in 2023 and 2024 exceeded the 2001-2020 averages.

DOC concentrations remained consistently low (<1.5 mg C l^{-1}). Shallow, lower-altitude lakes (e.g., STA, POZ, SFI, SAS) tended to have slightly higher DOC levels. DOC concentrations in 2023 and 2024 were within the range observed during 2001-2020.

Figure 4.5 Concentrations of the key parameters measured in lake surface waters during 2023 and 2024 and their means between 2013 and 2022.

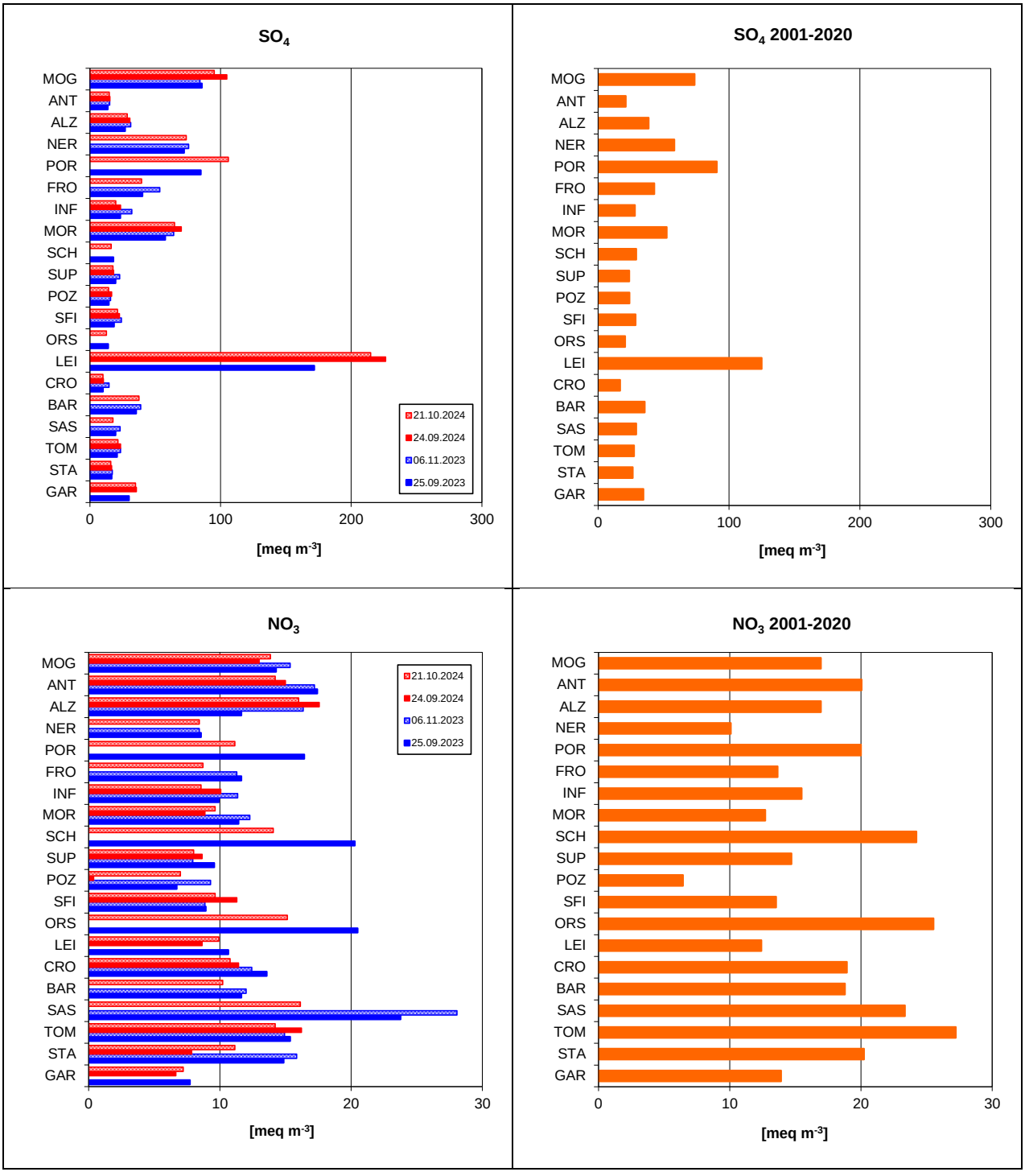

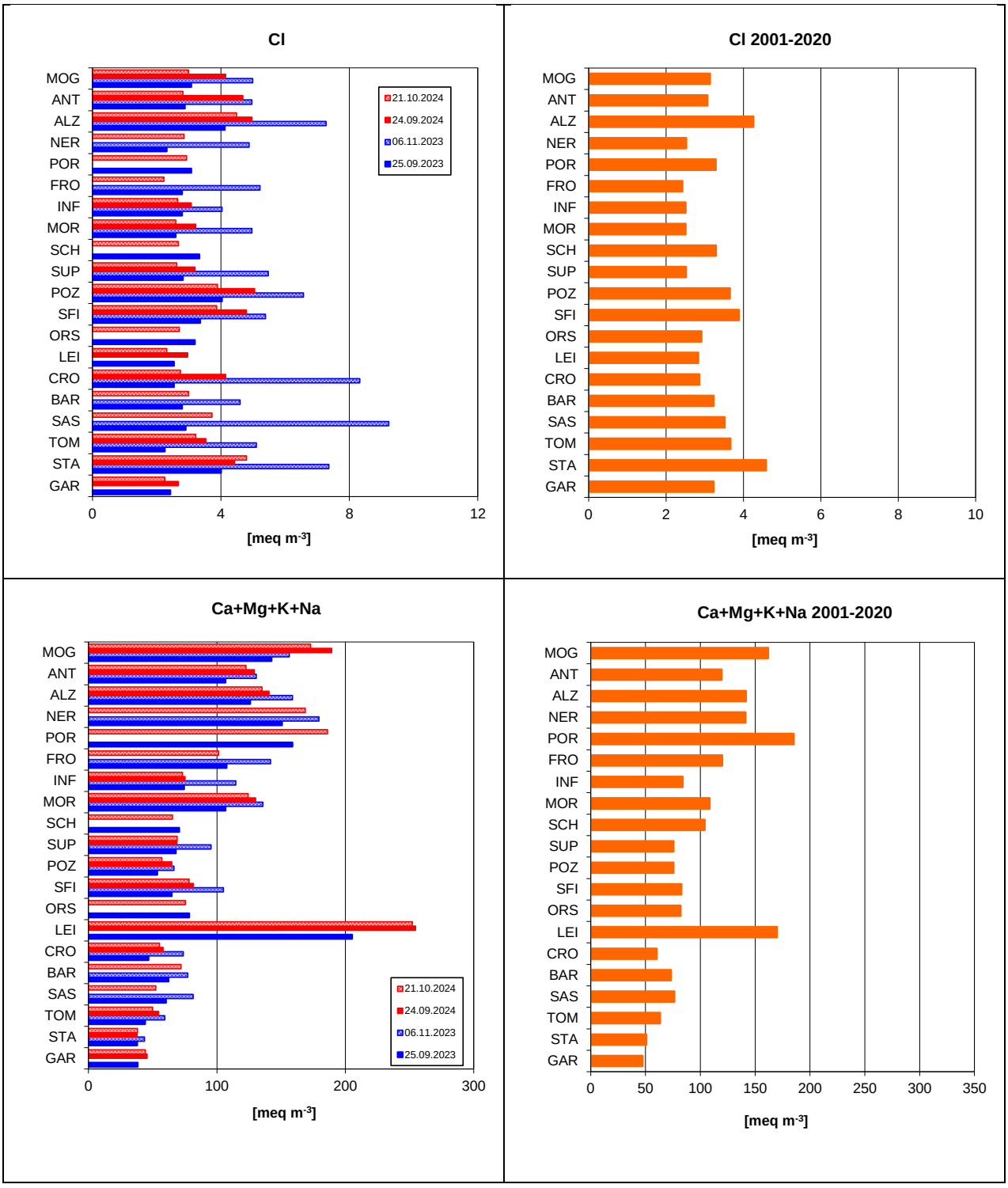
Cl
MOG
ANT
ALZ
NER
POR
FRO
INF
MOR
SCH
SUP
POZ
SFI
ORS
LEI
CRO
BAR
SAS
TOM
STA
GAR
21.10.2024
24.09.2024
06.11.2023
25.09.2023
0
4
8
12
[meq m-3]
Cl 2001-2020
0
2
4
6
8
10
[meq m-3]
Ca+Mg+K+Na
0
100
200
300
[meq m-3]
Ca+Mg+K+Na 2001-2020
0
50
100
150
200
250
300
350
[meq m-3]

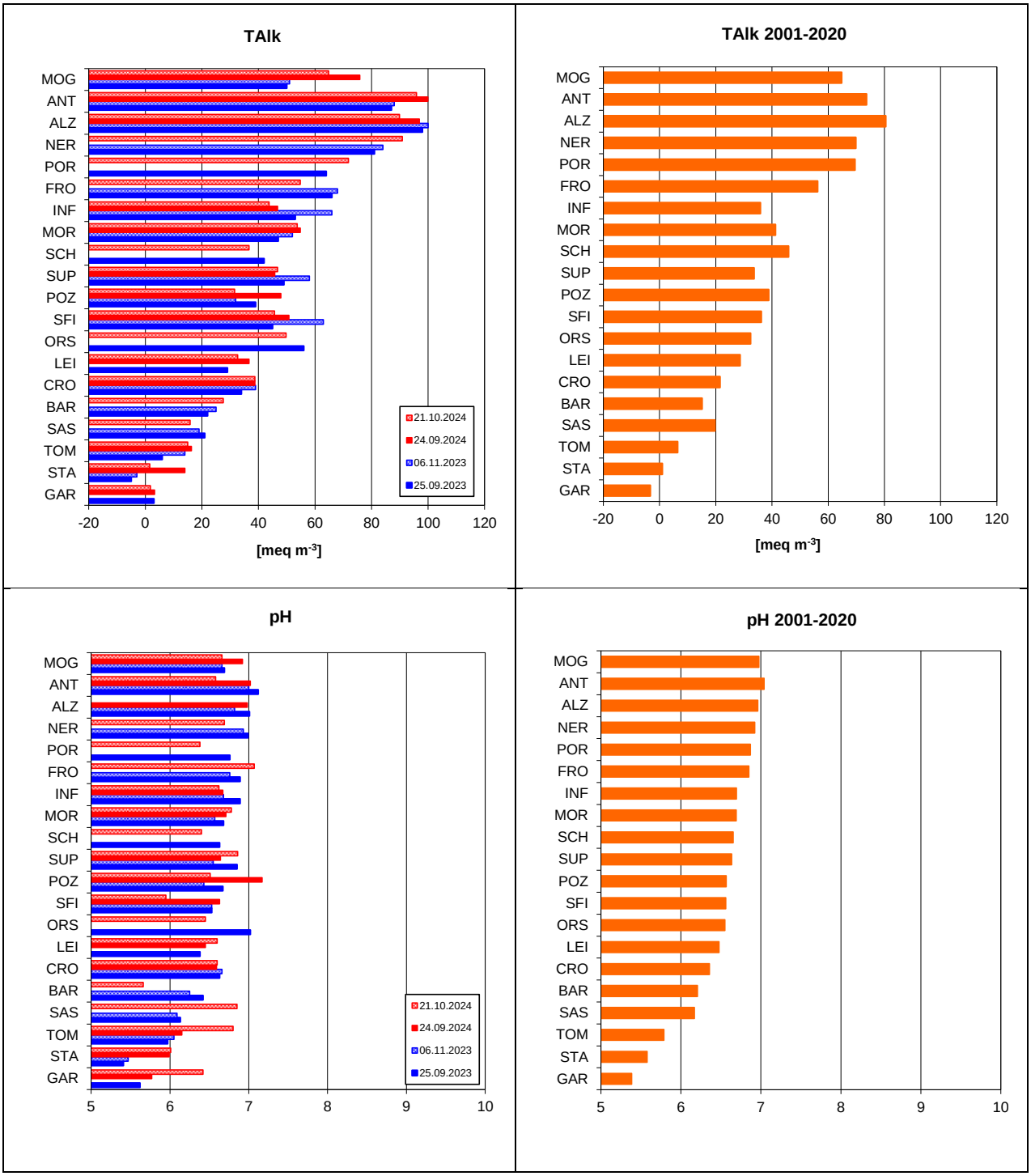
TAlk
MOG
ANT
ALZ
NER
POR
FRO
INF
MOR
SCH
SUP
POZ
SFI
ORS
LEI
CRO
BAR
SAS
TOM
STA
GAR
21.10.2024
24.09.2024
06.11.2023
25.09.2023
-20
0
20
40
60
80
100
120
[meq m-3]
TAlk 2001-2020
MOG
ANT
ALZ
NER
POR
FRO
INF
MOR
SCH
SUP
POZ
SFI
ORS
LEI
CRO
BAR
SAS
TOM
STA
GAR
-20
0
20
40
60
80
100
120
[meq m-3]
pH
MOG
ANT
ALZ
NER
POR
FRO
INF
MOR
SCH
SUP
POZ
SFI
ORS
LEI
CRO
BAR
SAS
TOM
STA
GAR
21.10.2024
24.09.2024
06.11.2023
25.09.2023
5
6
7
8
9
10
pH 2001-2020
MOG
ANT
ALZ
NER
POR
FRO
INF
MOR
SCH
SUP
POZ
SFI
ORS
LEI
CRO
BAR
SAS
TOM
STA
GAR
5
6
7
8
9
10

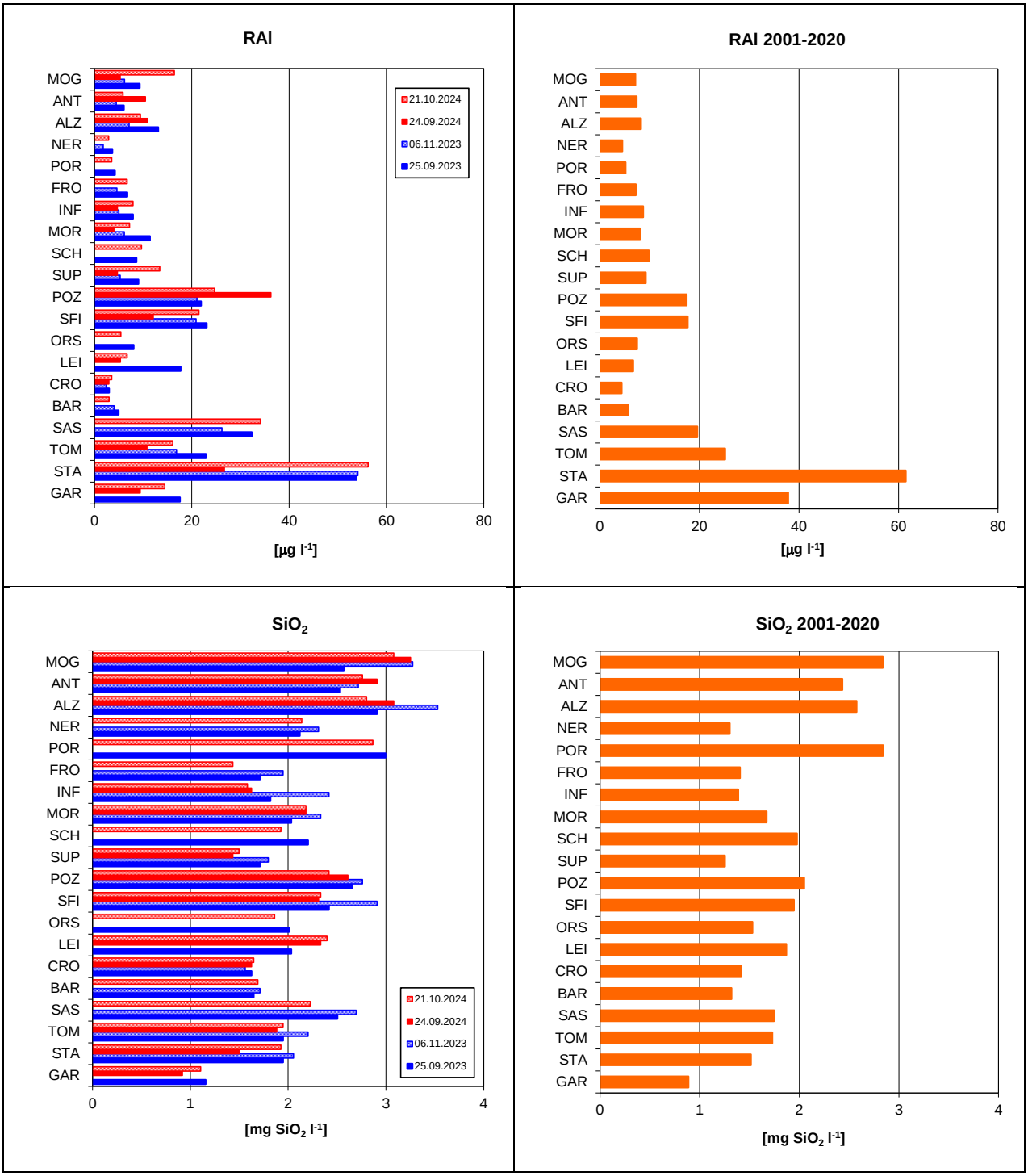
RAI
MOG
ANT
ALZ
NER
POR
FRO
INF
MOR
SCH
SUP
POZ
SFI
ORS
LEI
CRO
BAR
SAS
TOM
STA
GAR
21.10.2024
24.09.2024
06.11.2023
25.09.2023
0
20
40
60
80
[µg l-1]
RAI 2001-2020
MOG
ANT
ALZ
NER
POR
FRO
INF
MOR
SCH
SUP
POZ
SFI
ORS
LEI
CRO
BAR
SAS
TOM
STA
GAR
0
20
40
60
80
[µg l-1]
SiO2
MOG
ANT
ALZ
NER
POR
FRO
INF
MOR
SCH
SUP
POZ
SFI
ORS
LEI
CRO
BAR
SAS
TOM
STA
GAR
21.10.2024
24.09.2024
06.11.2023
25.09.2023
0
1
2
3
4
[mg SiO2 l-1]
SiO2 2001-2020
MOG
ANT
ALZ
NER
POR
FRO
INF
MOR
SCH
SUP
POZ
SFI
ORS
LEI
CRO
BAR
SAS
TOM
STA
GAR
0
1
2
3
4
[mg SiO2 l-1]

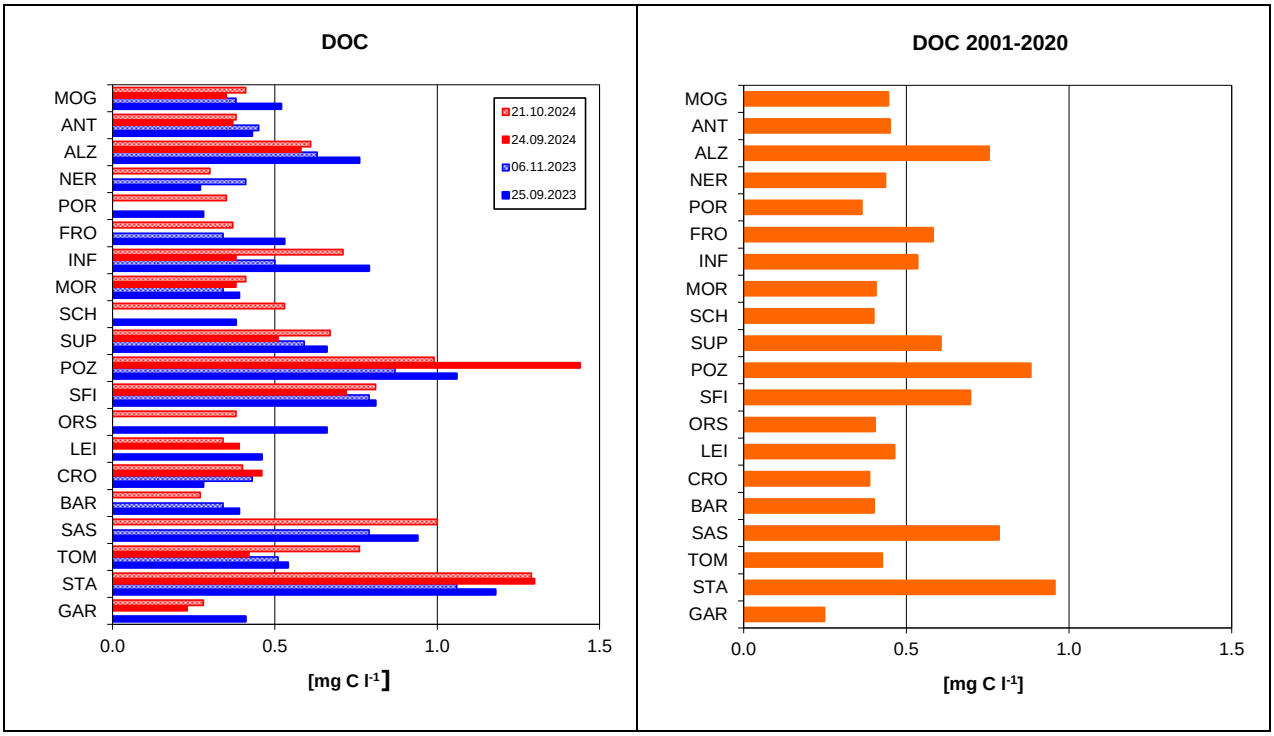
DOC
MOG
ANT
ALZ
NER
POR
FRO
INF
MOR
SCH
SUP
POZ
SFI
ORS
LEI
CRO
BAR
SAS
TOM
STA
GAR
21.10.2024
24.09.2024
06.11.2023
25.09.2023
0.0
0.5
1.0
1.5
[mg C l-1]
DOC 2001-2020
MOG
ANT
ALZ
NER
POR
FRO
INF
MOR
SCH
SUP
POZ
SFI
ORS
LEI
CRO
BAR
SAS
TOM
STA
GAR
0.0
0.5
1.0
1.5
[mg C l-1]

Figure 4.6 Concentrations of the key parameters in lake surface waters during 2023 and 2024 vs. their autumn means between 2001 and 2020.

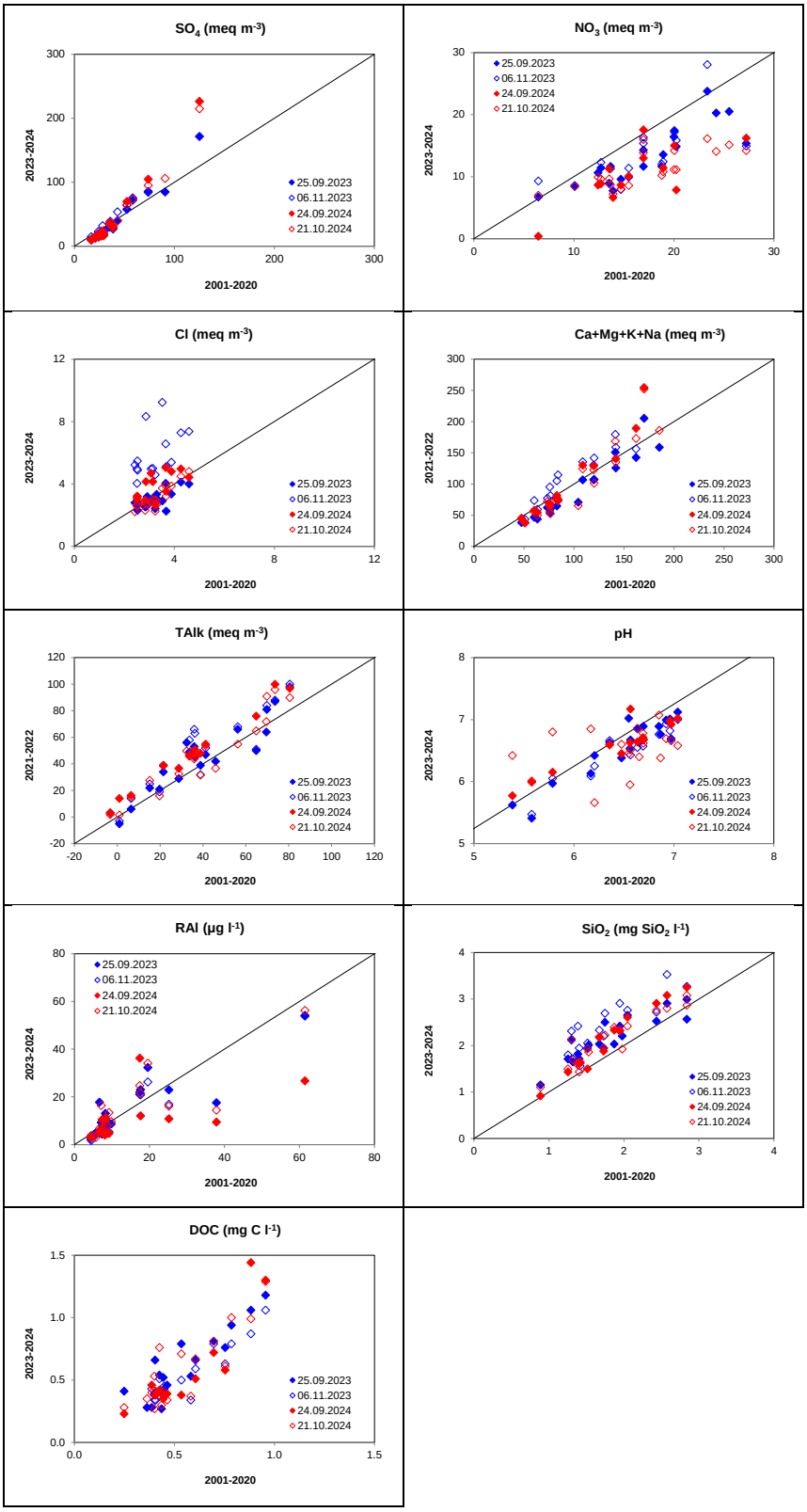

4.7.4 Long-term trends in lake water chemistry

Fig. 4.7 presents the concentrations of the key chemical parameters in lake surface water from the start of the monitoring to 2024. The results of the trend analysis, including Sen's slopes and the significance of observed trends, are summarized in Tab. 4.5. Most trends were evaluated for the period of continuous and consistent monitoring (2000–2024). However, due to changes in analytical methods, trends for RAl were assessed for 2013-2024, and those for DOC for 2011–2024.

SO_4 concentrations have decreased in the majority of lakes, with significant reductions observed in 13 out of 20 lakes from 2000 to 2024. The most pronounced decline occurred between 1990 and 2015, driven primarily by decreased SO_x emissions and the resulting reduction in SO_4 deposition. Nitrate (NO_3) concentrations showed significant declines in all lakes, reflecting reduced NO_x emissions, with the steepest decreases occurring between 2000 and 2015.

Consistent with catchment recovery from acidification, base cation concentrations (Ca, Mg, Na, K) have generally decreased, significantly so in 5 of the 20 lakes from 2000 to 2024. However, in five lakes (POR, LEI, MOR, MOG, and NER) SO_4 concentrations increased significantly, accompanied by positive trends in base cation concentrations. Four of these lakes (LEI, MOR, MOG, NER) are affected by thawing rock glaciers (Scapozza and Mari 2010), which are known to release SO_4, base cations, and various metals (Brighenti et al. 2024). Morandi et al. (2024) described the ion mobilization process in rock glaciers as a sequence of coupled steps: (i) rock glacier motion creating fresh fine-grained materials with reactive mineral surfaces, (ii) chemical weathering of these minerals, in particular the oxidation of sulfide, producing sulfuric acid and promoting the dissolution of solutes from the host rock (i.e., acid rock drainage), (iii) temporal storage and long-term enrichment of the dissolved solutes in rock glacier ice, (iv) final hydraulic mobilization during climate-change-induced accelerated degradation of rock glaciers. Supporting this theory, lakes LEI, MOR, and NER exhibited significant increases in SiO_2 concentrations, while lakes MOR and MOG also showed increases in RAl.

Reduced acidic deposition has led to significant increases in TAlk and pH across most lakes, irrespective of cryospheric influences. The most substantial reductions in hydrogen ion concentrations were observed in the three most acidic lakes, which also experienced the

largest declines in RAl concentrations: STA from 70–110 to 35–55 µg L^{-1}, TOM from 20–50 to 10–25 µg L^{-1}, and GAR from 25–60 to 10–20 µg L^{-1}.

The significant post-2013 increase in RAl concentrations in POZ and ALZ is more complex to interpret. Sterling et al. (2024) recently reported widespread and frequent reactive Al concentrations (RAl) that exceeded toxic thresholds in Nova Scotia rivers, despite high DOC concentrations, usually expected to reduce the bioavailability of Al by forming organo-Al complexes. They identified DOC as the strongest predictor (positive) of RAl concentrations. DOC in soil water can increase the release of Al via two mechanisms: (i) as an organic acid, DOC decreases soil pH, thereby increasing Al release; and (ii) by forming organic complexes with RAl. Sterling et al. (2024) suggested that the recruitment properties of DOC in soils might outweigh its protective properties in streams. In the same study, next to DOC, temperature was also positively correlated to RAl. Higher temperatures are thought to activate biological processes that mobilize Al from soils (Hendershot et al. 1986). Although the trends in DOC concentrations were mostly insignificant in the studied lakes, a negative correlation was observed between the Sen's slopes of DOC and the catchment mean altitude. This suggests that DOC concentrations are increasing in lower-altitude lake catchments, where the presence of soil and vegetation is higher. Excluding the most acidic lakes (STA, TOM, GAR), which exhibited the strongest decreases in H and RAl concentrations, as well as lakes likely influenced by thawing cryospheric features (POR, LEI, MOR, MOG, NER), where metal concentrations may be increasing, the remaining lakes showed a positive relationship between the Sen's slopes of DOC and RAl. These findings indicate that in lower-altitude lakes, concentrations of both DOC and RAl are increasing, likely as a consequence of climate change. The increase in DOC might help mitigate the rise in bioavailable and more toxic aluminium. However, since we do not directly RAl, we cannot confirm this with certainty.

Figure 4.7 Autumn concentrations of the key parameters in Alpine lakes from 1988 to 2024.

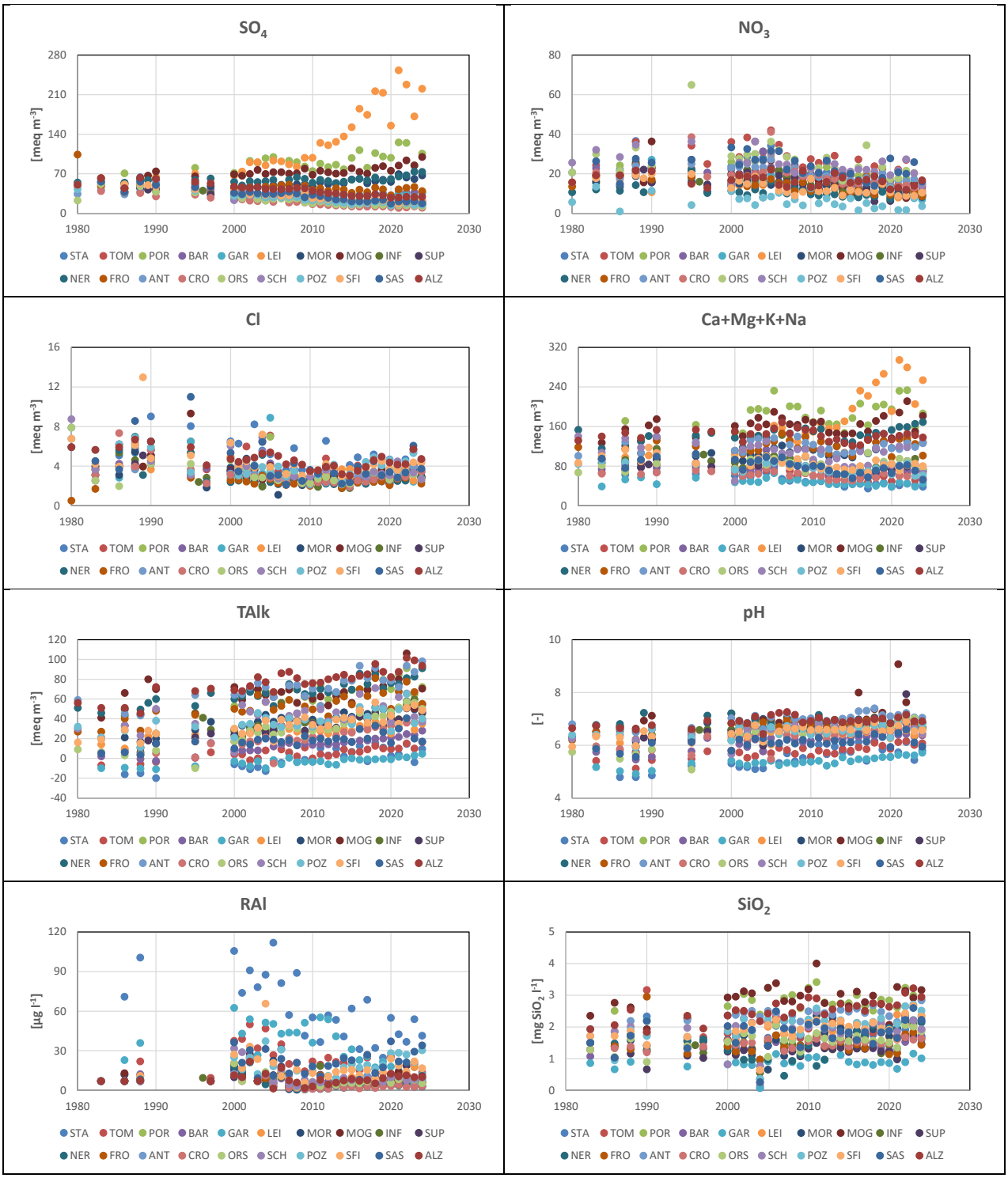

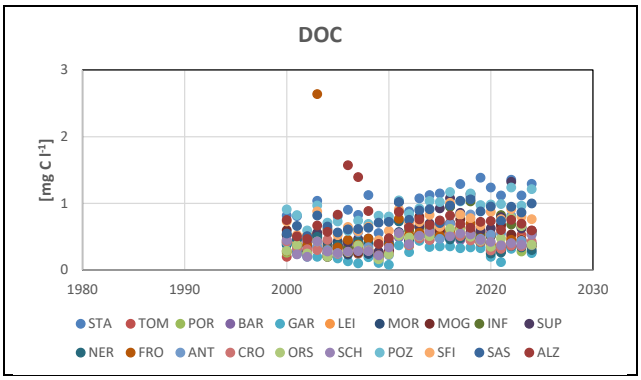

Table 4.5 Sen's slopes of the key parameters in Alpine lakes from 2000 to 2024, except RAl (2013-2024) and DOC (2011-2024). Red values indicate significant trends. SO_4. NO_3, Cl, Ca+Mg+K+Na, TAlk, ANC and H are expressed in meq m^{-3} yr^{-1}, SiO_2 and DOC in mg l^{-1} yr^{-1} and RAl in µg l^{-1} yr^{-1}.

Lake	pH	H	SO_4	NO_3	Cl	Ca+Mg+K+Na	TAlk	ANC	SiO_2	RAl	DOC
STA	0.030	-0.203	-0.98	-0.72	-0.03	-0.99	0.83	0.62	0.012	-0.44	0.024
TOM	0.018	-0.058	-0.59	-0.79	-0.01	-1.08	0.50	0.36	-0.003	-0.71	0.008
POR	0.005	0.001	0.93	-0.51	-0.02	0.58	0.71	0.27	0.000	-0.04	-0.005
BAR	0.014	-0.020	-0.18	-0.51	-0.03	-0.32	0.68	0.40	0.002	0.02	-0.008
GAR	0.017	-0.139	-0.19	-0.41	-0.04	-0.47	0.33	0.18	0.002	-2.02	-0.004
LEI	0.001	0.002	6.72	-0.23	-0.01	6.31	0.38	0.28	0.022	0.40	-0.007
MOR	0.004	0.001	0.80	-0.20	0.01	1.12	0.87	0.51	0.025	0.28	-0.007
MOG	0.002	0.003	0.73	-0.41	0.02	0.23	0.18	-0.20	-0.005	0.49	-0.005
INF	0.015	-0.004	-0.64	-0.52	0.00	-0.52	0.85	0.63	0.000	-0.09	0.003
SUP	0.018	-0.005	-0.61	-0.59	0.00	-0.29	1.04	0.77	0.006	0.23	-0.001
NER	-0.001	0.001	0.54	-0.12	0.00	1.03	0.88	0.60	0.060	0.10	-0.016
FRO	0.003	0.001	-0.18	-0.19	0.00	0.31	0.74	0.36	0.004	0.13	-0.011
ANT	0.010	0.001	-0.62	-0.40	-0.01	-0.29	1.00	0.65	0.010	0.17	0.010
CRO	0.016	-0.010	-0.65	-0.35	0.00	-0.28	0.96	0.68	0.007	0.06	-0.003
ORS	0.022	-0.009	-0.67	-0.53	-0.01	-0.12	1.43	1.14	0.004	0.29	0.002
SCH	0.006	0.001	-0.89	-0.26	-0.03	-1.10	0.45	-0.16	-0.002	0.07	-0.001
POZ	0.014	0.000	-0.80	-0.21	0.05	-0.77	0.47	0.22	0.012	1.54	0.019
SFI	0.007	0.001	-0.75	-0.21	0.00	-0.49	0.80	0.57	0.010	0.55	0.008
SAS	0.007	0.002	-0.86	-0.57	-0.02	-1.22	0.40	0.27	0.005	1.25	0.020
ALZ	0.001	-0.203	-0.90	-0.15	-0.02	-0.70	0.97	0.48	0.020	0.42	-0.002

4.8 River Verzasca

4.8.1 Hydrology

The discharge of the river Verzasca typically follows a seasonal pattern, with low flow conditions prevailing in winter, a pronounced increase in spring due to frequent precipitation and snowmelt, moderate discharge during summer, and elevated flow again in autumn (Fig. 4.8, monthly means 2001–2020). However, the monthly mean discharge in spring 2023 was lower than usual, while autumn 2023 and spring/summer 2024 experienced higher than average discharges (Fig. 4). Sampling coincided with high-flow events in May 2023 and April/May/June 2024.

Figure 4.8 Daily (red) and monthly (light blue) mean discharge of river VER during 2023 and 2024 and monthly mean dischare during 2001-2020 (dark blue). The vertical lines correspond to the sampling dates.

The discharge of VER at Sonogno has been estimated from the discharge at Lavertezzo (BWG 2001-2004 and BAFU 2005-2025).

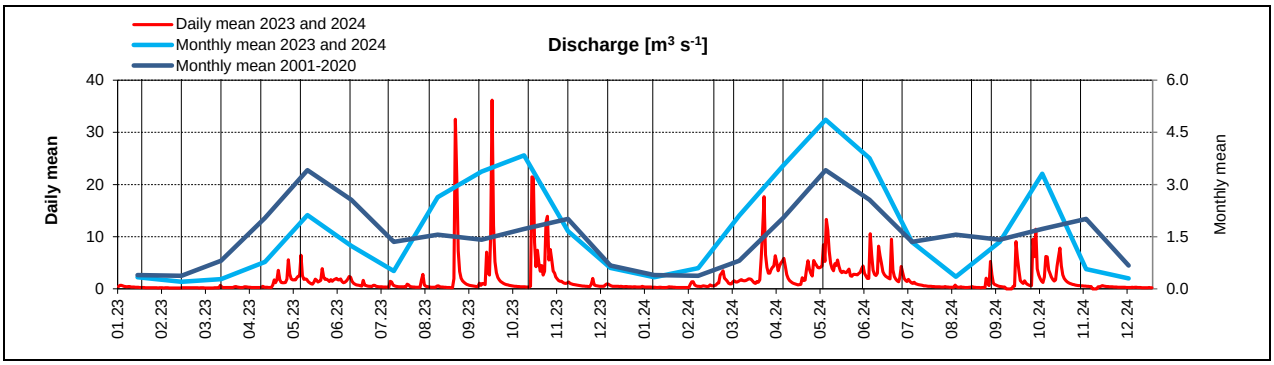

4.8.2 River water chemistry during 2023 and 2024 and monthly means of 2001-2020

The concentrations of SO_4, base cations (Ca, Mg, Na, K), Cl, TAlk, SiO_2, and pH in river Verzasca generally decrease during late spring and early summer when river discharge is highest, and increase throughout the rest of the year (Fig. 4.9, mean 2001–2020). Steingruber and Colombo (2006) attributed the observed seasonal patterns in SO_4, base cations, Cl, and SiO_2 to the dilution effects of rainwater and snowmelt, which contain lower concentrations of these solutes compared to surface waters. During rain events, river pH tends to decrease due to the acidity of precipitation, while TAlk is influenced by both dilution and consumption of acidity during these events

In contrast, NO_3 concentrations are typically elevated in winter, reach a peak in late spring during snow melt, and then decrease during summer, with episodic increases during high-flow events. These fluctuations are driven by a combination of factors: (i) reduced retention during colder months and during precipitation events, due to limited uptake by vegetation and algae and reduced denitrification, (ii) rapid release of accumulated NO_3 during snow melt in late spring, (iii) soil leaching during heavy precipitation events.

RAl concentrations are generally higher in spring and autumn when discharge is elevated, suggesting soil leaching, likely exacerbated by the lower pH during these periods.

DOC concentrations are lowest during the cold months when biological activity and the mineralization of organic matter are reduced.

Compared to the 2001–2020 averages, SO_4 and base cation concentrations in 2023 and 2024 were higher during periods of low discharge (due to reduced dilution) and lower during high discharge events. The opposite trend was observed for RAl and DOC.

NO_3 concentrations in 2023 and 2024 were lower than the monthly means from 2001–2020 for most months, suggesting a long-term decline. In contrast, TAlk and SiO_2 concentrations were higher. The lowest pH value (6.6) was recorded during a high-flow event in May 2024.

Figure 4.9 Concentrations of the main chemical parameters in river Verzasca during 2023 and 2024 and their average values during 2001-2020.

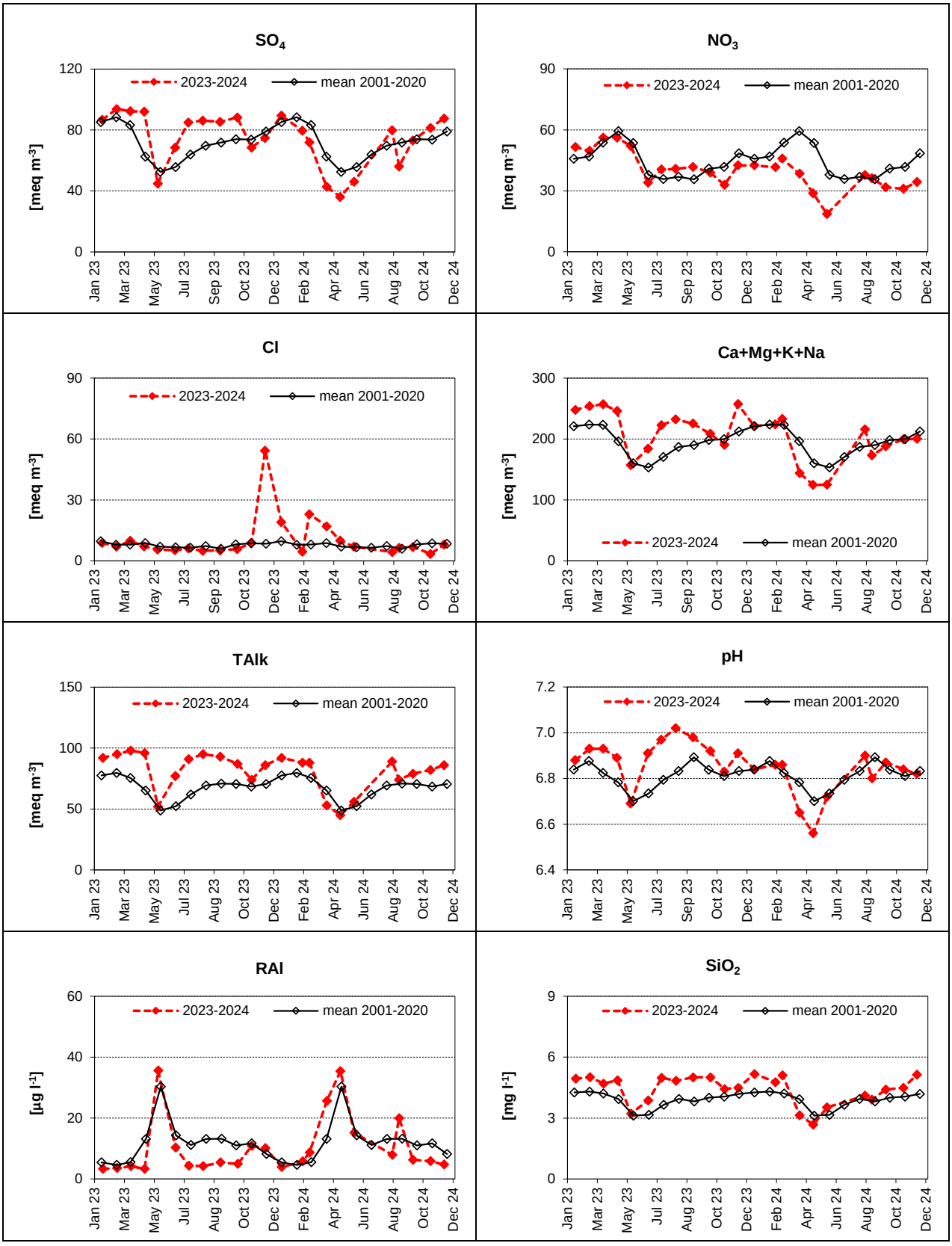

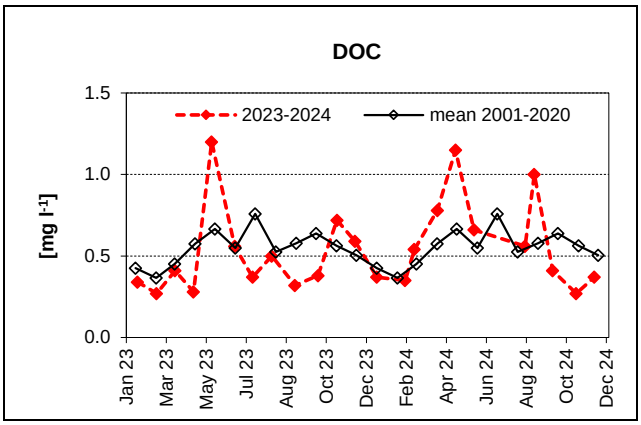

4.8.3 Temporal variations

Fig. 4.10 presents the concentrations of key parameters measured in river Verzasca from 2000 to 2024, with temporal trends detailed in Tab. 4.6.

Similar to the observations in lakes SO_4 and NO_3 concentrations in river Verzasca have decreased over time, leading to increases in TAlk and pH increased. The significant positive trend of SiO_2 after 2000 aligns with the observed increase in weathering activity, likely driven by climate change, as reported in various lakes.

Figure 4.10 Concentrations of the main chemical parameters in river Verzasca from 2000 to 2024

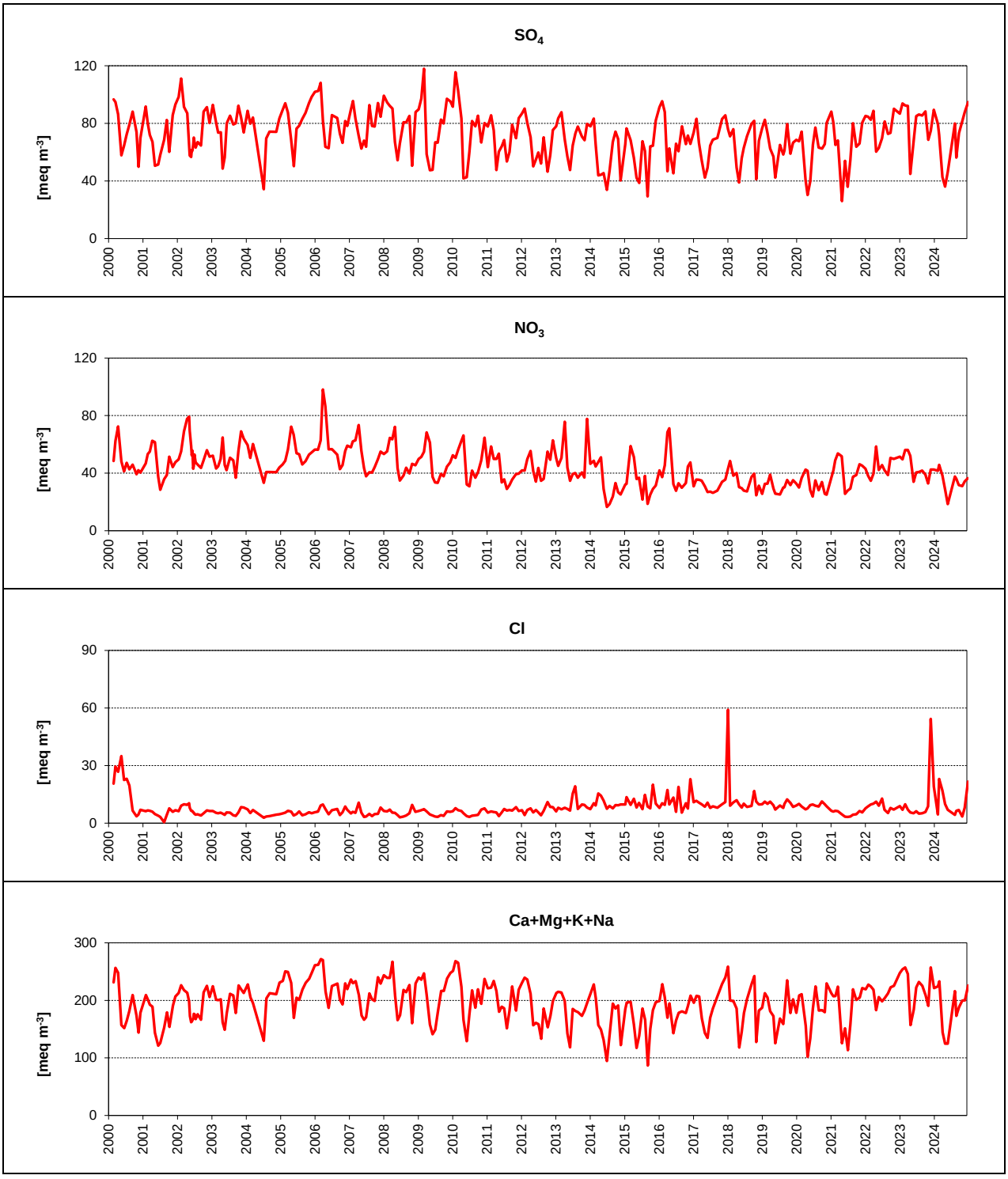

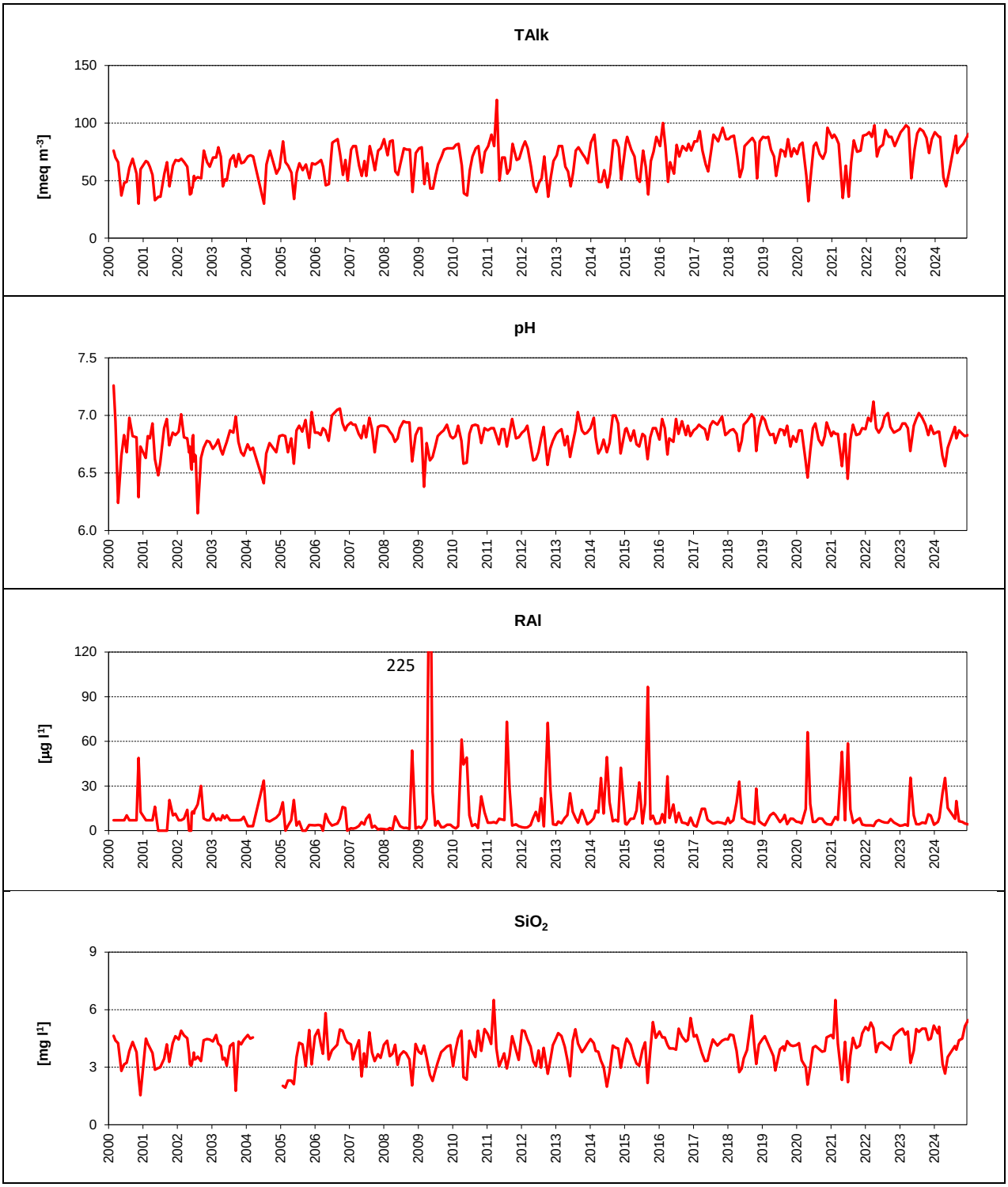
TAlk
[meq m-3]
150
100
50
0
2000 2001 2002 2003 2004 2005 2006 2007 2008 2009 2010 2011 2012 2013 2014 2015 2016 2017 2018 2019 2020 2021 2022 2023 2024
pH
7.5
7.0
6.5
6.0
2000 2001 2002 2003 2004 2005 2006 2007 2008 2009 2010 2011 2012 2013 2014 2015 2016 2017 2018 2019 2020 2021 2022 2023 2024
RAl
[µg l-1]
120
90
60
30
0
225
2000 2001 2002 2003 2004 2005 2006 2007 2008 2009 2010 2011 2012 2013 2014 2015 2016 2017 2018 2019 2020 2021 2022 2023 2024
SiO2
[mg l-1]
9
6
3
0
2000 2001 2002 2003 2004 2005 2006 2007 2008 2009 2010 2011 2012 2013 2014 2015 2016 2017 2018 2019 2020 2021 2022 2023 2024

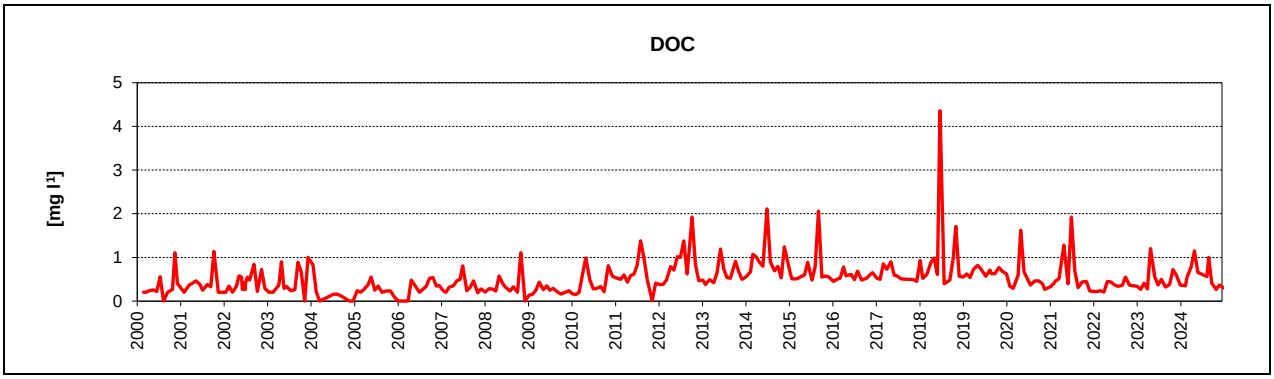

Table 4.6 Changes in concentrations (Sen's slopes) in river Verzasca during 2000-2024, except RAL (2013-2024) and DOC (2011-2024). Red values indicate significant trends. SO4. NO3, Cl, Ca+Mg+K+Na, TAlk, ANC and H are expressed in meq m^{-3} yr^{-1}, SiO_2 and DOC in mg l^{-1} yr^{-1} and RAl in µg l^{-1} yr^{-1}

River	Period	pH	H^+	SO_4	NO_3	Cl	Ca+Mg+K+Na	TAlk	ANC	RAL	SiO_2	DOC
VER	2000-2024	0.003	-1.0E-3	-0.51	-0.79	0.16	-0.34	1.00	0.68	-0.10	0.02	-0.02

5 Macroinvertebrates as bioindicators

5.1 Introduction

The primary objective of emission control programs is to achieve biological recovery. This includes the return of acid-sensitive species that had disappeared and the restoration of biological functions disrupted by acidification.

5.2 Methods

5.2.1 Sampling

Between 2000 and 2011, macroinvertebrates were regularly monitored in four lakes (INF, SUP, TOM, STA) and the rivers (Maggia (MAG), Vedeggio (VED) and Verzasca (VER)). Due to financial constraints, monitoring between 2012 to 2018 was limited to the most acid-sensitive sites (INF, SUP, TOM, STA, VER). Since 2019, only in the most acidic lakes TOM and STA monitoring continued.

Macroinvertebrates were sampled using the kick-sampling method, following the guidelines outlined in the ICP Waters Manual (Gundersen et al. 2025). Sampling typically tool place twice a year (in spring and in autumn). Until 2013, the samples were collected from both the littoral zone and the emissary. However, from 2014 onwards, only emissary samples were collected due to financial limitations. Emissaries were prioritized because they are more frequently inhabited by acidity-indicator species (Steingruber et al. 2013). Many of these species are rheophilic, making emissaries more suitable for assessing the impact of acidification.

Before to 2012, a single mixed sample from various substrates was taken at each site. From 2012 onwards, samples from fine and coarse substrates were collected separately. All macroinvertebrates specimens were preserved in 70% ethanol.

5.2.2 Identification

Taxonomic identification generally followed the guidelines of the ICP Waters Manual (Gundersen et al. 2025). However, in high-altitude Alpine lakes, chironomids often dominate the macroinvertebrate community; therefore, individuals from this family were identified to the species level.

Due to financial constraints, full taxonomic identification has been conducted every third year since 2021 (e.g., 2021, 2024).

5.2.3 Assessment approach

In Switzerland, the assessment of invertebrate samples from rivers is based on the standardized IBCH quality index (BAFU 2019), which evaluates taxonomic diversity (VT) and indicator groups (GI). The resulting index values range from 0 to 1. In this method, semi-quantitatively sampled invertebrates are identified primarily at the family level or at coarser taxonomic categories (e.g. oligochaetes). The IBCH_2019 index provides an overall evaluation of biological conditions in watercourses and classifying sites into five ecological condition classes:

- **Very good**: IBCH ≥ 0.8
- **Good**: 0.6 ≤ IBCH < 0.8
- **Moderate**: 0.4 ≤ IBCH < 0.6
- **Insufficient**: 0.2 ≤ IBCH < 0.4
- **Bad**: < 0.2)

While IBCH_2019 effectively highlights deficits in water quality and the habitat structure, its application to lakes in this study revealed limitations. Specifically, the index struggled to differentiate macroinvertebrate communities among high-altitude Alpine lakes with varying pH levels (Steingruber 2023). Currently, Switzerland lacks a dedicated indicator for acidification.

However, Steingruber et al. (2006) found that pH measurements in the rivers MAG, VED and VER corresponded well with the acidification classes developed by Braukmann and Biss (2004) for German mountain streams at mid altitude (400-1500 m a.s.l.) using macroinvertebrates as indicators. These classes are defined as follows:

1. **Continuously neutral:** pH 6.5 to >7.0, never below 6.0
2. **Predominantly neutral to episodically acidic:** pH 6.5 to 7.0, rarely below 5.5

3. **Periodically critically acidic:** pH 5.5 to 6.5, sometimes below

4. **Periodically strongly acidic:** pH around 5.5, periodically below

5. **Continuously extremely acidic:** pH 4.3 to 5.5, often below

However, these classes are not well-suited for assessing acidification in high-altitude lake outlets, where macrinvertebrate diversity is generally low, EPT taxa (Ephemeroptera, Plecoptera, Trichoptera) are scarce, and chironomids are abundant regardless of pH (Boggero and Lencioni 2006, Füreder et al. 2006, Steingruber et al. 2013). A general decline in EPT richness with increasing elevation and decreasing catchment area has also been reported by Altermatt et al. (2013).

Nonetheless, the Braukmann and Biss (2004) classification system could be adapted for use in high-altitude lake outlets. In the original method, indicator taxa are ranked according to their acid sensitivity (from 1 = highly acid-sensitive to 5 = very acid-resistant). Cumulative relative abundances are calculated until a threshold of 10% dominance is reached, with the indicator value of the last taxon added determining the acidification class. Steingruber et al. (2013) found that reducing the dominance threshold to 1% provided a better fit for high-altitude lake outlets.

In addition to indicator taxa, general invertebrate metrics - such as the total taxa number, EPT taxa number (particularly mayflies and stoneflies), and relative EPT abundance - have shown positive correlations with outlet pH (Steingruber et al. 2013). Moreover, there is some evidence that chironomid community composition changes during recovery from acidification, with species richness increasing over time (Orendt et al. 1999; Pinder and Morley 1995; Ruse 2011; Steingruber 2013).

5.2.4 Trend analysis

For the trend analysis, data from 2000 and 2001 were excluded because they included mixed samples from both the littoral zone and the emissary, making them unsuitable for direct comparison with the separately collected littoral and the outlet samples from 2002 onward. However, outlet samples collected in 2000 at lakes TOM and STA as part of the EMERGE project (European Mountain Lake Ecosystems: Regionalization, Diagnostic & Socio-Economic Evaluation) were included in the analysis.

o ensure consistency across years despite changes in taxonomic identification practices, a standardized identification level was defined for each taxonomic group. Information beyond this level was disregarded to avoid bias. The standardized identification levels were as follows:

- Annelida: class
- Arachnida: subcohort
- Coleoptera: genus
- Diptera: family (except Chironomidae, identified to species)
- Ephemeroptera: genus
- Heteroptera: genus
- Megaloptera: genus
- Odonata: genus
- Trichoptera: genus
- Mollusca: class
- Platyhelminthes: family

Moreover, to reduce biases related to sample size variability, rare taxa - defined as those with a relative abundance of ≤1% - were excluded from the trend analysis of taxonomic richness (total, EPT, and chironomid taxa). This approach helps mitigate the overrepresentation of rare species in larger samples and their underrepresentation in smaller ones.

To examine the influence of environmental parameters on temporal trends (2000-2024) in macroinvertebrate communities, Pearson correlation coefficient and their significance levels were calculated between various biological metrics – such as the relative abundances of individual taxa or taxa groups, total taxa, EPT and chironomid richness, and acidification classes – and a range of environmental parameters:

- **Average temperature** over the 2- and 5-month periods preceding and including the sampling month (T_3m, T_6m)
- **Sum of precipitation** over the 2- and 5-month periods preceding and including the sampling month (Prec_3m, Prec_6m)
- **Sum of Snowfall** (October–May)
- **pH and TAlk** (during summer and autumn sampling)
- **Time** (sampling year)

Temperature and precipitation data were obtained from the MeteoSwiss monitoring station at Robiei, and snowfall data were sourced from the WSL monitoring site at the same location.

5.3 Results and discussion

5.3.1 Lake chemistry

In autumn 2024, average concentrations of ANC were 10 µeq l^{-1} in STA and 12 µeq l^{-1} in lake TOM. Corresponding pH values were 5.8 in STA and 6.1 in TOM, while concentrations of RAl were 41 µg l^{-1} in STA and 13 µg l^{-1} in TOM. Over the monitoring period (2000-2024), both lakes exhibited significant increases in autumn ANC, pH and RAl (Fig. 5.1). In STA, ANC rose from an average of -10 to 10 µeq l^{-1} and pH from 5.2 to 5.7. In TOM, ANC increased from 0 to 15 µeq l^{-1}, and pH from 5.7 to 6.0. Over the same period, RAl concentrations significantly decreased in both lakes: in STA, from an average of 87 to 46 µg l^{-1}, and in TOM, from 41 to 20 µeq l^{-1}.

Figure 5.1 Autumn pH and RAl (in µg l^{-1}) in STA and TOM

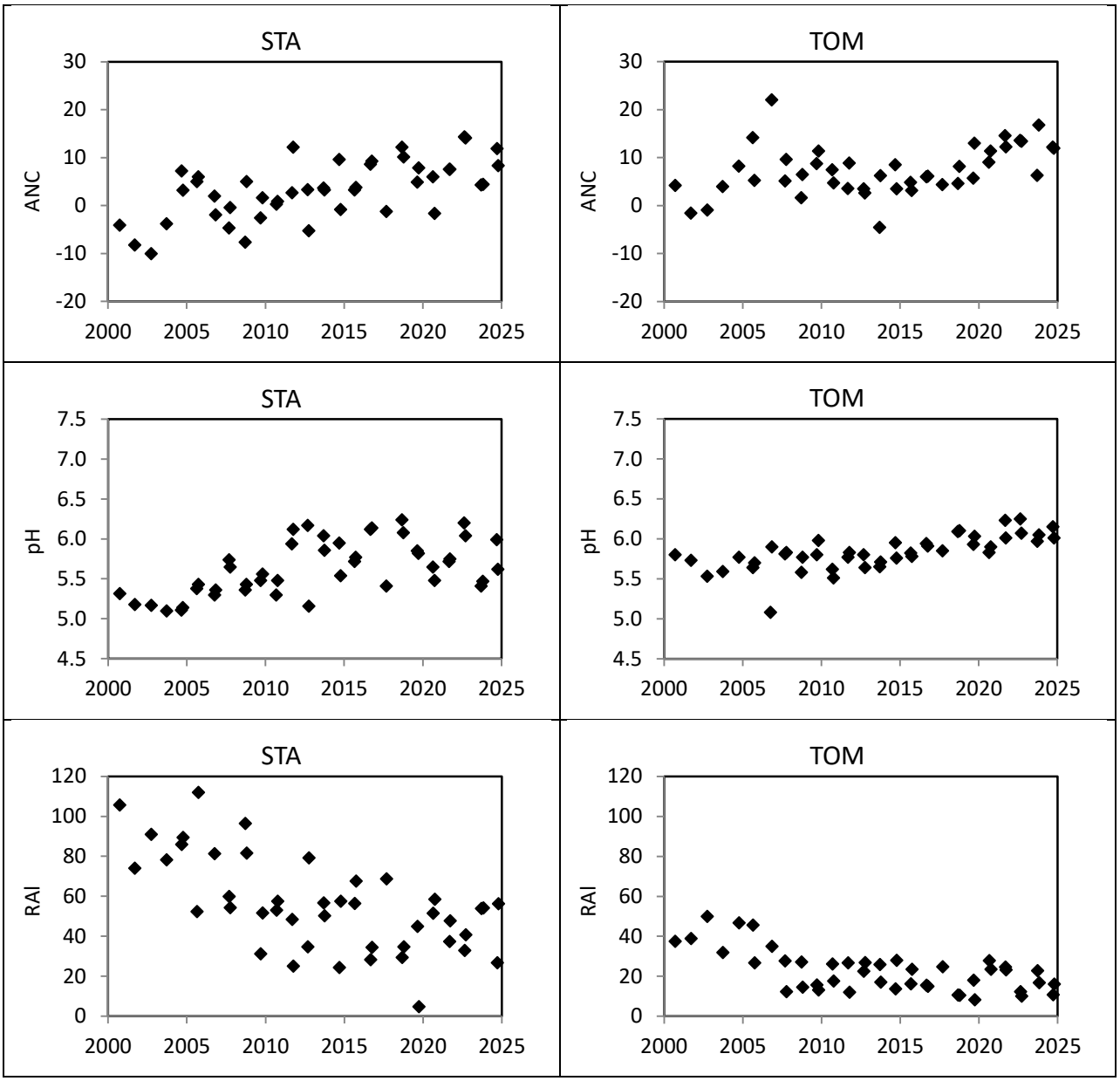

5.3.2 Macroinvertebrates in 2024

Macroinvertebrates samples were collected in June (TOM and STA), late September (STA) and at the beginning of October (TOM). The June samples from lake TOM contained very few individuals (Tab. 5.1), likely because the sampling took place slightly too early in the season - snow was still present along shorelines, and ice blocks were floating in the water.

Table 5.1 Lake sample size during 2024

LAKE OUTLETS	MONTH	Fine substrate	Coarse substrate
TOM	June (4.6.2024)	449	128
	October (5.10.2024)	3028	1810
STA	June (28.6.2024)	1051	1427
	September (28.9.2024)	1494	1377

The relative abundances of the main taxa and acidification indexes are shown in Table 5.2. In lake STA the most abundant taxonomic groups were Chironomidae, followed by other Diptera (including *Ceratopogonidae* and *Simuliidae* on coarse substrate), Nemathelminthes, and Oligochaeta. In lake TOM, the dominant groups were Chironomidae and Oligochaeta, followed by Nemathelminthes. The generally very acid sensitive Ephemeroptera were absent in both lakes.

As regards Plecoptera and Trichoptera, only acid-tolerant species were identified. In TOM, these included *Leuctra sp.*, *Nemoura mortoni*, *Plectrocnemia sp*., and *Ryacophila sp.*. Similarly, in STA, *Nemoura cinerea*, *Plectrocnemia sp.* and *Ryacophila sp..* Odonata were found exclusively in STA, likely due to its wetland character, as it is a small, shallow lake, with wetland vegetation.

Among Chironomidae, Othocladiinae were the dominant subfamily in STA, followed by Chironominae (Tanytarsini) and Tanypodinae (Pentaneurini). The most common species were *Psectrocladius octomaculatus, Psectrocladius sordidellus* and *Corynoneura scutellata-group.* In TOM, the chironomid community was dominated by Chironominae (*Chironomini and Tanytarsini*) and Orthocladiinae, followed by Tanypodinae (*Pentaneurini*). The most abundant species were *Polypedilum nubeculosum*, *Psectrocladius octomaculatus*, *Trissopelopia longimana* and *Paratanytarsus austriacus*.

Consistent with the water chemistry, the invertebrate communities – classified according to the acidification classes of Braukmann and Biss (2004) – indicted that lake TOM had slightly

less acidic conditions (ranging from periodically strongly acidic to periodically critically acidic) compared to lake STA, which was classified as continuously extremely acidic to periodically strongly acidic.

Table 5.2 Relative abundance and number of taxa in lake outlets on different substrates during 2024.
0.0% indicate values >0.0% but < 0.05%. * modified Braukmann and Biss class

TAXA	TOM				STA			
	Fine		Coarse		Fine		Coarse	
	Spring	Autumn	Spring	Autumn	Spring	Autumn	Spring	Autumn
OLIGOCHAETA	**28.5%**	**55.9%**	**8.6%**	**19.9%**	**12.7%**	**4.7%**	**2.4%**	**12.8%**
Enchitraeidae	4.0%	0.1%	6.3%	0.3%	4.6%	1.3%	0.6%	0.7%
Lumbriculidae	1.6%	1.0%		0.1%	0.8%	3.1%	0.3%	0.1%
Naididae/Tubificidae	22.9%	54.8%	2.3%	19.5%	7.3%	0.3%	1.5%	11.8%
Other								0.1%
HYDRACARINA		**1.5%**		**0.1%**	**1.0%**	**1.7%**	**0.1%**	**0.5%**
COLEOPTERA		**0.1%**		**0.1%**				
Agabus sp.		0.1%		0.1%				
Platambus sp.		0.0%						
DIPTERA (Chironomidae)	**46.8%**	**30.7%**	**50.8%**	**66.4%**	**12.7%**	**70.9%**	**49.9%**	**52.1%**
Endochironomus dipar-Gr.						0.1%		
Pagastiella orophila					*0.3%*	0.1%		
Polypedilum nubeculosum-Gr.	20.0%	1.9%	35.2%	9.5%				1.2%
Micropsectra contracta							0.1%	
Micropsectra sp.	0.2%	1.8%		2.8%				
Paratanytarsus austriacus	0.7%	8.3%	2.3%	11.9%				
Paratanytarsus dissimilis Gr.					0.9%		3.6%	
Paratanytarsus sp.							0.1%	0.2%
Pseudodiamesa branickii							0.1%	
Chaetocladius piger-Gr.			0.8%					
Corynoneura scutellata Gr.	4.5%		0.8%		6.5%		10.5%	0.2%
Corynoneura sp.	0.2%	1.7%	0.8%	1.7%				
Heterotanytarsus marcidus		0.1%		0.2%		0.1%		0.1%
Psectrocladius barbimanus							0.2%	0.1%
Psectrocladius octomaculatus	11.8%	9.9%	6.3%	6.1%	5.0%	46.9%	21.0%	36.3%
Psectrocladius sordidellus-Gr.		0.1%	1.6%	16.6%		23.4%	14.0%	10.9%
Trissopelopia longimana	8.9%	6.6%	2.3%	16.6%		0.3%		
Zavrelimyia mel.				0.1%			0.1%	
Zavrelimyia sp.	0.4%	0.5%	0.8%	1.0%				3.0%
Procladius sp.						0.1%		
DIPTERA (Other)	**0.7%**	**0.2%**	**2.3%**	**4.3%**	**36.2%**	**15.7%**	**42.5%**	**18.1%**
Ceratopogonidae	0.4%	0.0%	0.8%		36.1%	13.5%	14.9%	8.2%
Chaoboridae						0.5%		0.4%
Empididae				0.1%				
Limoniidae	0.2%							
Simuliidae		0.2%	0.8%	4.1%	0.1%	1.7%	27.6%	9.5%
Tipulidae			0.%	0.1%				
MEGALOPTERA	**0.2%**	**0.7%**						**0.2%**
Sialis fuliginosa	0.2%	0.1%						
Sialis sp.		0.6%						0.2%
ODONATA					**1.9%**	**1.7%**	**0.6%**	**1.0%**
Aeshna juncea					0.3%	0.1%	0.1%	0.1%
Aeshna sp.					0.2%	1.1%		0.7%
Enallagma cyatigerum					0.5%		0.2%	
Coenagrionidae					0.6%			
Cordulidae					0.2%	0.2%	0.2%	
Somatochlora alpestris								0.1%
Somatochlora sp.					0.2%	0.3%	0.1%	0.1%
PLECOPTERA	**5.8%**	**1.4%**	**3.1%**	**6.0%**	**0.1%**		**0.9%**	**3.5%**
Leuctra sp.	5.1%	1.3%	3.1%	5.2%				
Nemoura cinerea					0.1%		**0.9%**	

Nemoura mortoni				0.8%				
Nemoura sp.		0.1%						
Nemurella pictetii	0.7%							
Nemuridae								3.5%
TRICHOPTERA		**0.2%**		**1.9%**			**0.4%**	**7.6%**
Limnephlidae		0.2%		1.6%				
Plectrocnemia sp.				0.1%			0.4%	1.7%
Policentropodidae		0.1%						6.0%
Rhyacophila sp.				0.2%				
Other								
NEMATHELMINTHES	**18%**	**9.2%**	**35.2%**	**1.2%**	**35.4%**	**5.3%**	**3.2%**	**4.1%**
TURBELLARIA				**0.1%**	**0.1%**	**0.1%**		
Planariidae					0.1%	0.1%		
Number total taxa	16	23	15	24	16	18	20	20
Number EPT taxa	2	4	1	5	1	0	2	2
Rel. abundance EPT taxa	5.8%	1.6%	3.1%	7.9%	0.1%	0.0%	1.3%	11.1%
Mean acidification class*	4	4	5	5	4	4	3	4

5.3.3 Long-term patterns in macroinvertebrates communities (2000 to 2024)

From 2000 to 2024. Chironomidae were the most abundant macroinvertebrate family in both lakes, representing 53% of individuals in STA and 45% in TOM. In lake STA the next most common families were Ceratopogonidae (17%), Nemouridae (8%), and Simuliidae (7%). In lake TOM, Simuliidae (21%), Leuctridae (18%), and Oligochaeta (6%) followed Chironomidae in abundance.

Focusing specifically on chironomids:

- In lake STA, the most abundant genera were Psectrocladius sp. (23%), Paratanytarsus sp. (23%), Corynoneura sp. (19%), Micropsectra sp. (14%), and Heterotrissocladius sp. (7%).
- In lake TOM, Polypedilum sp. (42%) dominated, followed by Trissopelopia sp. (21%), Corynoneura sp. (14%), and Psectrocladius sp. (7%).

Significant seasonal differences were observed in several taxa, likely influenced by water chemistry (e.g., lower pH and temperatures due to snowmelt in early summer) and species-specific life cycles.

In lake STA the relative abundances of Nemouridae, Odonata, and overall EPT taxa, as well as the number of EPT genera, were higher in autumn than in summer. Among chironomids,

Orthocladiinae species such as *Heterotrissocladius marcidus* and *Corynoneura sp.* were more abundant in summer.

In lake TOM Simuliidae showed significantly higher relative abundances in autumn. Among chironomids Chironomini (*Polypedilum nubeculosum*) were more abundant in summer, while Tanypodinae (*Trissopelopia longimana*), Orthocladiinae, and Tanytarsini (*Micropsectra sp.*) prevailed in autumn.

In both lakes, the Swiss IBCH water quality index was significantly higher in autumn compared to spring.

Despite improvements in water chemistry, none of the analyzed biological indicators suggested a clear recovery of the macroinvertebrate communities from acidification (Fig. 5.2).

- In lake TOM, the total number of taxa and the number of EPT and chironomid genera remained unchanged.
- In lake STA, the number of EPT genera was stable, but total taxa richness declined due to a reduction in chironomid genera.
- The acidification class according to Braukmann and Biss (2004) also showed no long-term improvement. In lake TOM, values fluctuated between class 3 (periodically critically acidic) and class 5 (continuously extremely acidic); in lake STA, between class 4 (periodically strongly acidic) and class 5.
- The IBCH index similarly showed no consistent positive trend. It ranged from 0.4 to 0.6 in lake TOM (moderate ecological quality) and from 0.0 to 0.6 in lake STA (ranging from poor to moderate quality, typically 0.4–0.6 in autumn).

Interestingly, in lake TOM, the relative abundance of EPT taxa appeared to decline over time, primarily due to the decreasing abundance of Leuctridae (*Leuctra sp*.) (Fig. 5.3). This decline coincided with an increase in the cumulative abundance of Oligochaeta, Chironomidae, Simuliidae, and Hydracarina.

In lake STA, the relative abundance of EPT taxa remained consistently low, with only occasional autumn peaks in Nemouridae (*Nemoura sp*.).

Figure 5.2 Macroinvertebrate metrics

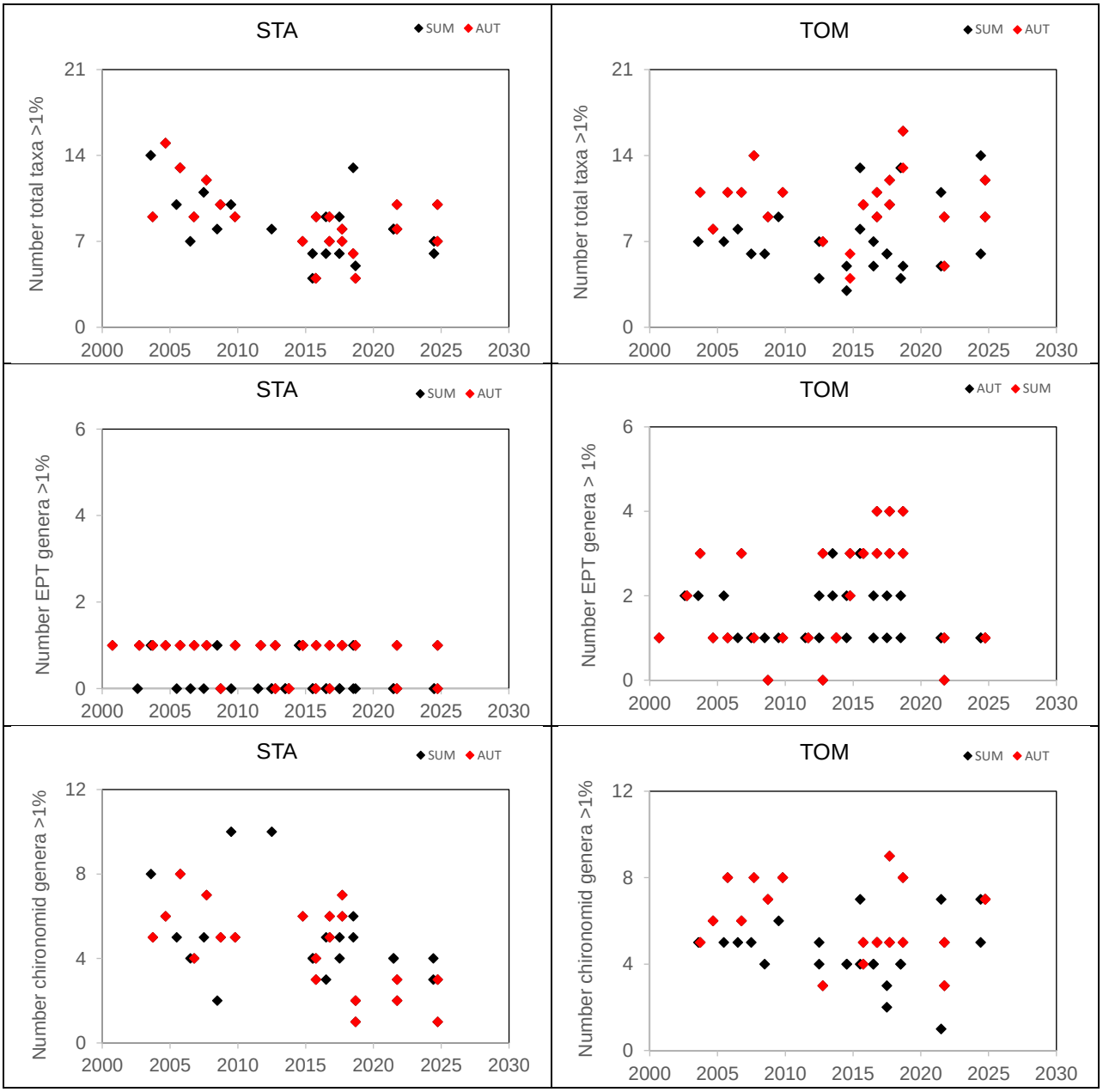

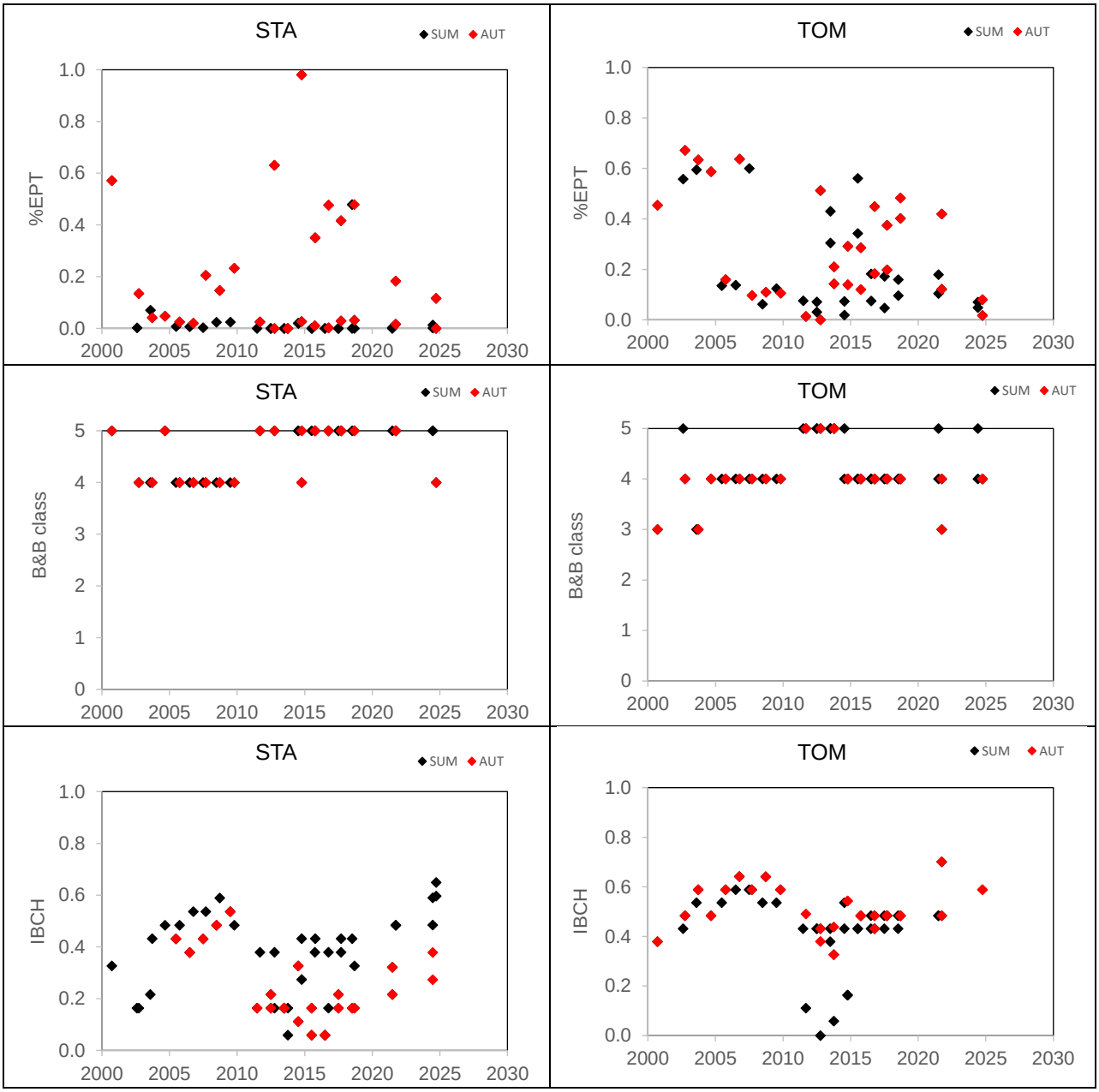
STA
SUM
AUT
%EPT
TOM
SUM
AUT
%EPT
STA
SUM
AUT
B&B class
TOM
SUM
AUT
B&B class
STA
SUM
AUT
IBCH
TOM
SUM
AUT
IBCH

Figure 5.3 Temporal trends of not chironomid taxa in lakes STA and TOM.

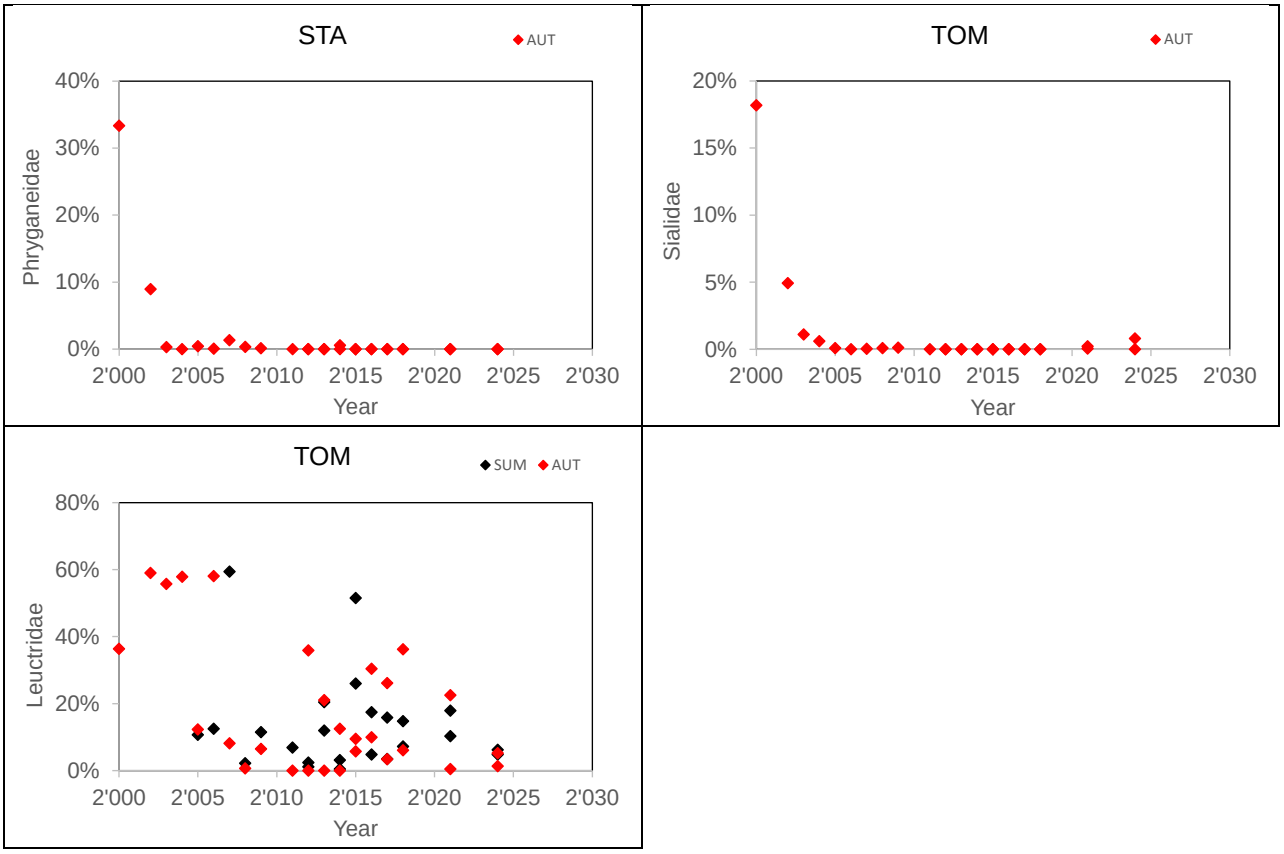

Although the analyzed metrics do not indicate a recovery of the macroinvertebrate communities from acidification, the distribution of certain taxa has changed significantly over time (Fig. 5.3 and Fig. 5.4).

For example, Phryganeidae (*Hagenella clathrata*), a species typically associated with raised bogs, has not been recorded in lake STA since 2014. Similarly, Sialidae (*Sialis fuliginosa*), has shown a significant decline in lake TOM. The causes behind these changes remain unclear.

Time-related trends were also observed for several chironomid species in both lakes.

In both STA and TOM, the relative abundance of *Psectrocladius sp*. (primarily *P. limbatellus*, *P. sordidellus*, and *P. octomaculatus*) increased over time. In autumn samples, these increases correlated positively with pH (Pearson correlation coefficients: STA = 0.69; TOM = 0.52), suggesting that the gradual rise in pH may have contributed to their increased abundance.

Conversely, the relative abundance of *Corynoneura sp*. (mainly *C. lobata* and *C. scutellata*) declined over time in both lakes. In autumn samples, their abundance showed a negative correlation T_6m (STA = -0.51; TOM = -0.53), indicating a possible sensitivity to increasing air temperatures.

Paratanytarsus sp. (mainly *P. austriacus*) exhibited diverging trends: decreasing in STA but increasing in TOM. In STA, abundance was strongly negatively correlated with T_6m (-0.71), while in TOM it was more closely associated with pH (0.60). Given the similar surface water temperatures, but significantly lower concentrations of aluminum in TOM, it is possible that the improved water chemistry in TOM had a stronger influence on *Paratanytarsus sp*. than the negative effects of warming.

Additionally, in lake STA, *Endochironomus dispar* declined in autumn, and *Heterotrissocladius marcidus* declined in summer. The decline of *E. dispar* was negatively correlated with pH (-0.55), suggesting it may be sensitive to improving water quality. *H. marcidus* showed negative correlations with both TAlk (-0.47) and T_6m (-0.59), indicating that both chemical recovery and rising temperatures could be affecting its population.

However, despite the observed temporal trends in certain taxa and their correlations with environmental variables, we cannot assert with certainty the existence of causal relationships. What we can state with reasonable confidence is that macroinvertebrate communities have undergone changes since the beginning of monitoring in 2000.

Because we lack data on the composition of invertebrate communities prior to acidification, it remains unclear whether the observed changes represent a recovery toward pre-acidification conditions. The analysis of subfossil chironomid remains in sediment cores would be a valuable approach to reconstruct historical community compositions.

However, recent studies, while occasionally reporting biological recovery marked by the return of more acid-sensitive species, do not observe a re-establishment of pre-acidification communities, even in water bodies showing clear chemical recovery (Belle and Johnson 2024, Diamond et al. 2022). These findings suggest that, in addition to acidification recovery, other factors—particularly the growing influence of climate change—are shaping community

dynamics (Belle and Johnson 2024). As a result, a complete return to pre-acidification conditions appears increasingly unlikely.

Figure 5.4 Temporal trends of chironomid taxa in lakes STA and TOM.

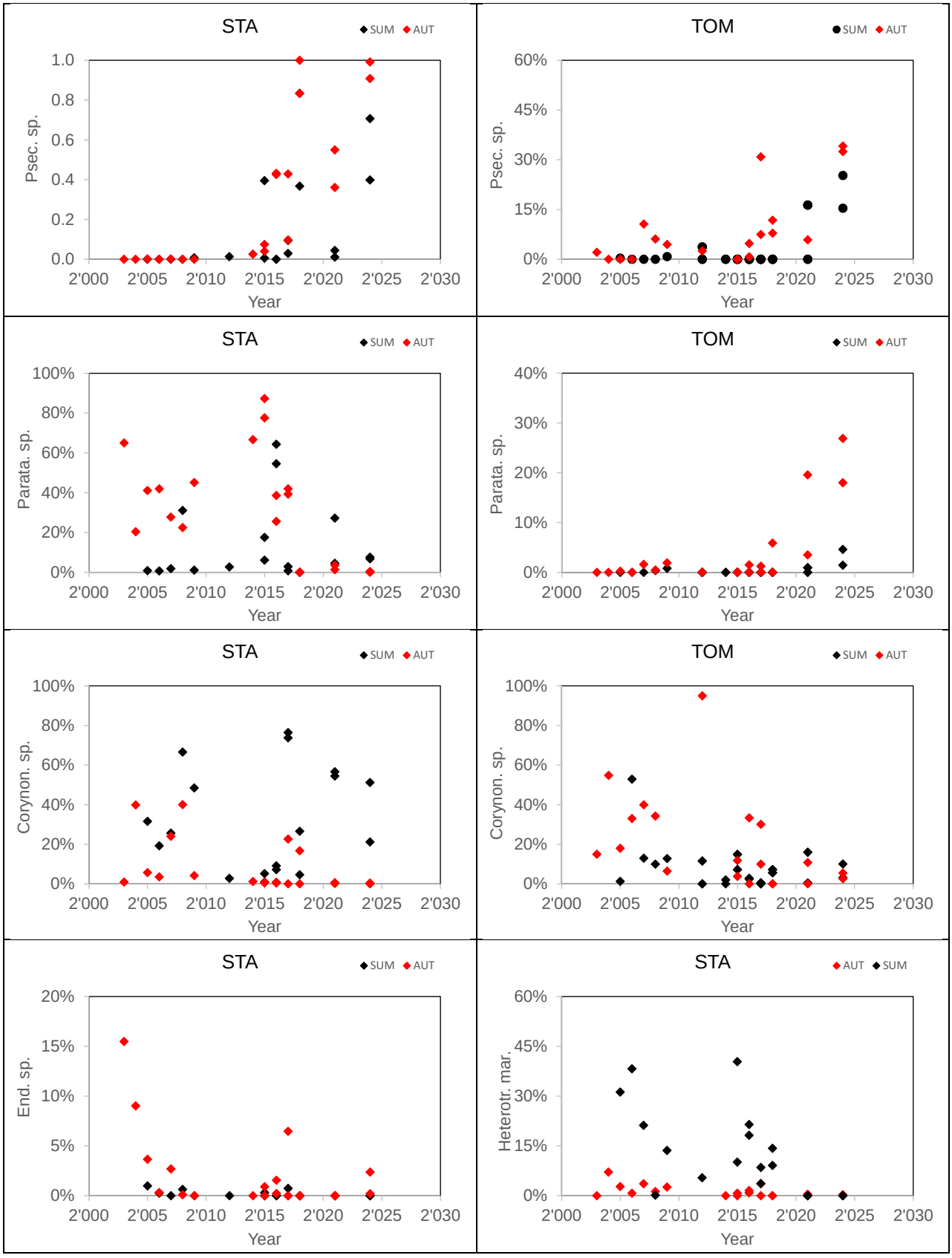

Bibliography

Altermatt F., Seymour M. and Martinez N. 2013. River network properties shape -diversity and community similarity patterns of aquatic insect communities across major drainage basins. J. Biogeogr. 40: 2249-2260.

BAFU (Ed.). 2019. Methoden zur Untersuchung und Beurteilung von Fliessgewässern (IBCH_2019). Makrozoobenthos-Stufe F. Umwelt-Vollzug Nr. 1026. Bundesamt für Umwelt. Bern.

Belle S. and Johnson R.K. 2024. Acidification of freshwater lakes in Scandinavia: impacts and recovery of chironomid communities under accelerating environmental changes. Hydrobiologia 851: 585-600.

Boggero A. and Lencioni V. 2006. Macroinvertebrates assemblages of high altitude lakes, inlets and outlets in the southern Alps. Arch. Hydrobiology 165: 37-61.

Braukmann U. and Biss R. 2004. Conceptual study-An improved method to assess acidification in German streams by using benthic macroinvertebrates. Limnologica 34: 433-450.

Brighenti S., Colombo N., Wagner T., Pettauer M., Guyennon N., Krainer K., Tolotti M., Rogora M., Paro L., Steingruber S.M., Del Siro C., Scapozza C., Sileo N.R., Villarroel C.D., Hayashi M., Munroe J., Trombotto Liaudat D., Cerasino L., Tirler W., F. Comiti, Freppaz M., Salerno F., Iggy Litaor M., Cremonese E., Morra di Cella U., Winkler G. 2024. Factors controlling the water quality of rock glacier springs in European and American mountain ranges. Sci. Total Environ. 953: 175706

BAFU (Ed.). 2005-2025. Hydrologisches Jahrbuch der Schweiz 2004-2024. Bundesamt für Umwelt, Bern.

BWG (Ed.). 2001-2004. Hydrologisches Jahrbuch der Schweiz 2000-2003. Bundesamt für Wasser und Geologie, Bern.

CLRTAP. 2024. Manual on methodologies and criteria for modelling and mapping critical loads and levels and air pollution effects risks and trends - Mapping critical loads for ecosystems, Chapter V. UNECE Convention on Long-range Transboundary Air Pollution.

Diamond S.E., Harvey R., Heathcote A., Lini A. and Morales-Williams A.M. 2022. Decoupling of chemical and biological recovery from acidification in a montane lake, Vermont, USA. Journal of Paleolimnology 68(4): 427–442.

Evans C.D., Monteith D.T., Fowler D., Cape J.N. and Brayshaw S. (2011). Hydrochloric Acid: An Overlooked Driver of Environmental Change. Environ. Sci. Technol. 45: 1887–1894.

Füreder L., Ettinger E, Boggero A., Thaler B. and Thies H. 2006. Macroinvertebrate diversity in Alpine lakes: effects of altitude and catchments properties. Hydrobiologia 562: 123-144.

Gilbert R.O. 1987. Statistical methods for environmental pollution monitoring. John Wiley & Sons, New York, 336 pp.

Gundersen C.B. et al. 2025. ICP Waters Programme Manual. NIVA report 8047-2025. ICP Waters Report 158/2025. Norwegian Institute for Water Research, Oslo, 107 p.

Hedin L.O., L. Granat, G.E. Likens, H. Rodhe. 1990. Strong similarities in seasonal concentration ratios of SO_4^{2-}, NO_3^- and NH_4^+ in precipitation between Sweden and the northeastern US. Tellus 423B: 454-462.

Hendershot W.H., Courchense F., Jeffreis D.S. 1996. Aluminum geochemistry at the catchment scale in watersheds influenced by acidic precipitation. In: Sposito G. (Ed.) The environmental Chemistry of aluminium. Lewis Publishers. NY.

Hirsch R.M. and J.R. Slack. 1984. A nonparametric test for seasonal data with serial dependence. Water Resources Research 20: 727-732.

Hirsch R.M., J.R. Slack and R.A. Smith. 1982. Techniques of trend analysis for monthly water quality data. Water Resources Research 18: 107-121

Mann H.B. 1945. Nonparametric tests against trend. Econometrics 13: 245-249.

Marchetto A. 2015. rkt: Mann-Kendall test, Seasonal and Regional Kendall Tests. (last update 19.3.2015).

MeteoSvizzera. 2024. Bollettino del clima dell'anno 2023. Ufficio federale di meteorologia (MeteoSvizzera).

MeteoSvizzera. 2025. Bollettino del clima dell'anno 2024. Ufficio federale di meteorologia (MeteoSvizzera).

Morandi H., Furrer G., Margrethz M., Mair D., Wanner C. Massive mobilization of toxic elements from an intact rock glacier in the central Eastern Alps. The Cryosphere 18: 5153-5171.

Orendt C. 1999. Chironomids as bioindicators in acidified streams: a contribution to the acidity tolerance of chironomid species with a classification in sensitivity classes. Internat. Rev. Hydrobiol. 84: 439-449.

Pinder L.C.V. and Morley D.J. 1995, Chironomid as indicators of water quality – with a comparision of the chironomid fauna of a series of contrasting cumbriam tarns. In: Harrington R. and Stork N.E. (eds.) Insects in a changing environment. Academic Press. London, 271-293 pp.

Posch M., Eggenberger U., Kurz D. and Rihm B. 2007. Critical loads of acidity for Alpine lakes. A weathering rate calculation model and the generalized First-order Acidity Balance (FAB) model applied to Alpine lake catchments. Environmental studies no. 0709. Federal Office for the Environment (FOEN), Berne, 69pp.

Ruse l. 2011. Lake acidification assessed using chironomid pupal exuviae. Fudam. Appl. Limnol. 178: 267-286.

Scapozza C. and S. Mari. 2010. Catasto, caratteristiche e dinamica dei rock glaciers delle Alpi Ticinesi. Bollettino della Società ticinese di Scienze naturali 98: 15-29.

Steingruber S. 2023. Biological responses to reduced acidification in surface waters in Switzerland. In: Velle et al. (Eds.) Responses of benthic invertebrates to chemical recovery from acidification. NIVA report SNO 7881-2023. ICP Waters Report 153/2023. Norwegian Institute for Water Research, Oslo: 47-55.

Steingruber S.M., Boggero A., Pradella Caissutti C., Dumnicka E. and L. Colombo. 2013. Can we use macroinvertebrates as indicators of acidification of high-altitude Alpine lakes? Bollettino della Società ticinese di Scienze naturali 101: 23-34.

Steingruber S. and L. Colombo. 2006. Impact of air pollution on Alpine lakes and rivers. Environmental studies no. UW-0619. Federal Office for the Environment. Berne, 74 pp.

Sterling S.M., MacLeod S., Rotteveel L., Hart K., Clair T.A, Halfyard E.A., O'Brian N.L. 2020. Ionic aluminum concentrations exceed thresholds for aquatic health in Nova Scotian rivers, even during conditions of high dissolved organic carbon and low flow. Hydrol. Earth Syst. Sci. 24: 4763-4775.

US EPA. 2018. Final aquatic life ambient quality criteria for aluminum-2018. EPA-022-R-18_001. Washington, D.C.

Wright R.F., Dale T., Gjessing E:T, Hendrey G.R., Henriksen A., Johannessen M. and Muniz I.P. 1975. Impact of acid precipitation on freshwater ecosystems in Norway. Water, Air Soil Poll. 6: 483-499.

Wright R.F. and Jenkins A. 2001 Climate change as a confounding factor in reversibility of acidification: RAIN and CLIMEX projects. Hydrol. Earth. Syst. Sci. 5: 477-486.

Acknowledgments

This study was commissioned and partially financially supported by the Federal Office for the Environment (FOEN).